Muscle *Bmal1* is necessary for normal transcriptomic and metabolomic adaptation to endurance exercise training.

Author Information

Mark R Viggars[1,2]*, Hannah E Berko[1,2], Miguel A Gutierrez-Monreal[1,2], Ryan A Martin[1,2], Karyn A Esser[1,2,*].

Affiliations

[1]Department of Physiology and Aging, University of Florida, Gainesville, Florida United States.

[2]Myology Institute, University of Florida, Gainesville, Florida, United States.

Author contributions

M.V, K.A.E designed experiments. M.V, H.E.B performed experiments. M.V, R.A.M, M.A.G, K.A.E interpretations and analysis. M.V, K.A.E wrote and reviewed the final manuscript. All authors contributed to the research of the published work and have read and approved the final version of the manuscript.

Declaration of Interests: The authors declare no competing interests.

Keywords: Exercise, circadian clock, skeletal muscle, transcription, oxidative phosphorylation, glycolysis.

Corresponding author

Correspondence to: Mark R Viggars m.viggars@ufl.edu ORCID: 0000-0002-0722-7051.

Karyn A Esser kaesser@ufl.edu ORCID 0000-0002-5791-1441.

Physical Address: Department of Physiology and Aging, University of Florida, Gainesville, Florida United States.

Abstract

Objective: The skeletal muscle circadian clock plays a pivotal role in muscle homeostasis and metabolic flexibility. Recently, this clock mechanism has been linked to both transcriptional and metabolic responses to acute exercise. However, the contribution of the circadian clock mechanism to the molecular and phenotypic adaptations to exercise training have not been defined.

Methods: Inducible skeletal muscle-specific Bmal1-floxed mice were treated with tamoxifen to induce skeletal muscle specific deletion of Bmal1 (iMSBmal1KO) or given a vehicle. Mice were assigned to normal cage conditions, or 6-weeks of progressive treadmill training. Exercise performance, body composition, and tissue/serum indices of metabolic health were assessed over the timecourse of training. Gastrocnemius muscles were collected 48-hours after their last exercise bout for histological, biochemical, and molecular analyses including RNA-sequencing and untargeted metabolomics.

Results: Improvements in exercise workload and maximal performance were comparable between iMSBmal1KO mice and vehicle treated controls after 6-weeks of exercise training. However, exercise training in the absence of *Bmal1* was not able to rescue the metabolic phenotype and hyperinsulinemia of the iMSBmal1KO mice, attributed to the continued dysregulation of core clock components and gene expression relating to glucose metabolism. Importantly, a much larger and divergent transcriptional reprogramming occurred in the muscle of iMSBmal1KO mice in comparison to their vehicle treated counterparts. This response included a large compensatory upregulation of genes associated with fatty acid β-oxidation, pyruvate metabolism, citric acid cycle components and oxidative phosphorylation components, including mitochondrial subunits and mitoribosome units.

Conclusions: Collectively, we propose that endurance training requires muscle *Bmal1*, and the core clock network, to elicit well recognized molecular adaptations. In the absence of *Bmal1*, exercise training results in a much larger and divergent re-networking of the basal skeletal muscle transcriptome and metabolome. We also demonstrate that skeletal muscle *Bmal1* is indispensable for the transcriptional regulation of glucose homeostasis, even after a 6-weeks exercise training programme.

Keywords

Muscle metabolism, circadian rhythms, transcription, BMAL1, exercise adaptation, amino acids.

1. Introduction

Physical exercise brings about acute mechanical and metabolic changes within skeletal muscle, often considered as signals to invoke adaptation [1]. With longer periods of training, skeletal muscle becomes more accustomed to repeated bout of exercise through alterations in chromatin accessibility and transcription factor activity which alter the basal steady state transcriptome. Dependent on the exercise modality, these changes can support increases in muscle size, improved metabolism and proteostasis, altered contractile properties, as well as changes in mitochondrial and ribosomal content [2,3].

Circadian transcription factors and their autoregulatory transcription-translation feedback loops (TTFL) regulate skeletal muscle homeostasis through diurnally rhythmic and non-rhythmic gene expression and through regulation of chromatin[4–7]. The skeletal muscle TTFL also temporally primes muscle metabolism for oxidation during the inactive phase and regulates a shift in substrate preference to glycolysis/ glucose utilisation during the active phase [5,8–11]. With loss of the clock, as seen in the inducible muscle-specific Bmal1KO model, we and others[4,9,12] have previously reported that these mice become glucose intolerant, hyper insulinemic and have elevated non-fasting blood glucose across the day attributed to defective skeletal muscle glucose uptake and metabolism [9].

A clear interaction between exercise and the circadian TTFL has been established in recent years. The negative limb of the circadian TTFL is known to be responsive to acute exercise/muscle contraction (e.g., *Pers*, *Nfil3*, *Dbp*) [13–18] and exercising at different times of the day is known to lead to unique metabolomic and transcriptional perturbations following an acute exercise bout [19–22]. Exercise training has also been linked to an enhancement of the circadian transcriptome, by increasing the number of diurnally oscillating genes [23,24]. Various measures of exercise performance such as strength and endurance capacity also present time-of-day differences [24–27].

While it is clear that exercise and the skeletal muscle circadian TTFL are inextricably linked [28], the role, if any, a functional skeletal muscle clock has on skeletal muscle adaptation to exercise has yet to be elucidated. Here we assess the importance of the endogenous skeletal muscle TTFL for exercise adaptation through ablation of *Bmal1* expression in adult myofibers, essentially terminating the core circadian TTFL [5]. The molecular and phenotypic changes downstream of loss of muscle BMAL1 have been well described previously[4,5,8,9,12,23,29].

We assessed a number of parameters associated with exercise performance, body composition, behaviour, and indices of metabolic health from skeletal muscle, liver, blood, and serum. We also performed transcriptomic and global metabolomic analysis of the gastrocnemius muscle to elucidate how the basal or steady state transcriptome and metabolome remodels itself after exercise training in the absence of BMAL1. Our data identified that BMAL1, and likely the core clock mechanism, is a required component for the normal exercise training molecular adaptations. In the

absence of BMAL1, exercise training resulted in a larger and divergent transcriptional and metabolomic remodelling of the steady state within skeletal muscle. Our mechanistic insights into the interplay between the skeletal muscle circadian TTFL and exercise training adaptation further highlight the important link between the skeletal muscle clock and metabolic regulation.

2. Materials and Methods

2.1. Ethical approval

All animal and experimental procedures in this study were conducted in accordance with the guidelines of the University of Florida for the care and use of laboratory animals (IACUC #201809136). The use of animals for exercise protocols was in accordance with the ARRIVE guidelines and guidelines established by the US Public Health Service Policy on Humane Care and Use of Laboratory Animals.

2.2. Mouse model

Male inducible skeletal muscle-specific *Bmal1* knockout mice were generated as previously described [5,8,9]. Skeletal muscle-specific tamoxifen inducible Cre recombinase mice were bred in-house at the University of Florida. This mouse has a Cre recombinase flanked by two mutated oestrogen receptors, driven by a human skeletal muscle actin promoter. Cre recombinase mice were crossed with the Bmal1-floxed mouse also bred in house, but originally acquired through Jackson Labs (B6, 1294(Cg)-Arntl tm1Weit/J), to generate the inducible skeletal muscle-specific Bmal1-floxed mouse (iMSBmal1$^{fl/fl}$). Activation of Cre recombination was performed by intraperitoneal injections of tamoxifen (2 mg/day) dissolved in sunflower seed oil for five consecutive days when the mice reached ~4 months of age. These mice are referred to as iMSBmal1KO mice henceforth. Controls were Cre$^{+/-}$:Bmal1$^{fl/fl}$ mice treated with a vehicle (15 % ethanol in sunflower seed oil) and are referred to as Vehicle mice from this point forward.

To assess recombination specificity within the gastrocnemius, DNA was extracted from ~1-5mg of muscle post-mortem, lysed in tail lysis buffer (10mM Tris pH 8, 100mM NaCl, 10mM EDTA, 0.5% SDS and 20mg/ml of Proteinase K) and DNA purified using the DNeasy Blood and Tissue Kit (Qiagen, Venlo, Netherlands). PCR was performed with extracted DNA and primers for the recombined and non-recombined alleles as previously described [8]. The PCR reaction was run on a 1.5% agarose gel (0.0005% ethidium bromide) to visualize the DNA products. Recombination specificity is provided in supplementary figure 1.

21 male mice were randomly assigned to tamoxifen or vehicle treatment, with or without exercise training at ~11 months of age. For clarity, these groups will be referred to in future text as Vehicle Control (n=5), Vehicle Exercise Trained (n=5), iMSBmal1KO Control (n=6), and iMSBmal1KO Exercise Trained (n=5). Mice were single housed in conditions of 23 ± 1.5°C, 58 ± 5.8% relative humidity within temperature and humidity controlled light boxes. Light schedules were

maintained on a 12:12 h light: dark schedule with *ad libitum* access to standard rodent chow (Envigo Teklad 2918, Indianapolis, IN, USA) and water. The macronutrient content of this chow is 24% protein, 18% fat and 58% carbohydrate, presented as a percent of calorie intake. To maintain standardised nomenclature for this study, we will reference time through use of zeitgeber time (ZT), were ZT0 refers to time of lights on and ZT12 refers to time of lights off. The active period of the day for mice is from ZT12-ZT24 and their rest period is ZT0-ZT12. All treadmill familiarization and training sessions were performed in the active phase so transportation of mice from housing to the treadmill room was in a light tight cart and the treadmill room was dark with red lights. A summary of the experimental design can be found in Figure 1A.

2.3 Graded treadmill exercise testing

Mice from all groups were first subjected to treadmill familiarization under red light on a Panlab treadmill (Harvard Apparatus, Holliston, MA) at ZT13. Familiarization consisted of 3 sessions performed on 3 consecutive days. The first familiarization session started at 10 cm/s for 5 min at 0° incline. The incline was then adjusted to 5° and speed was increased by 2 cm/s every 2 min up to 20 cm/s (15 minutes total). The second day consisted of an increase in speed every 3 min by 3 cm/s from 10 cm/s to 24 cm/s at an incline of 10°, (18 minutes total). The final familiarization session was the same as the second but performed at a 15° incline, (18 minutes total).

Following 1 day of rest, mice were subject to a maximal capacity test to serve as a baseline performance measure, conducted at ZT13 under red light. For the maximal capacity test, animals began at a speed of 10 cm/s at 10° incline for a 5 min warm-up. From which the incline was increased to 15° and the treadmill speed increased by 3 cm/s every 2 min until exhaustion. The treadmill was operated with the electrical shock grid turned off and mice gently encouraged by a compressed air canister when needed. Mice were deemed to be exhausted when they remained in contact with the back of the treadmill >15 s and could not be encouraged to move away by the compressed air.

Mice in groups assigned to exercise training were given 2-weeks of rest before their 6-weeks of exercise training commenced. Exercise training was always completed at ZT13 under red light, 5 times per week for a total of 30 individual exercise training bouts. Each bout consisted of 1 hour of treadmill running at 100% of work done (group mean), calculated according to previous work [30], work done = ($M \cdot D \cdot \sin q$). M is the mass (g) of the animal, D is the distance (m) ran in the maximal capacity test and sin q is the slope (15°) of the treadmill. Work done is measured in arbitrary units. For each training session, the slope of the treadmill was kept at 15° and the speed was adjusted to correspond to 100% of maximal capacity of the most recent maximal capacity test. Additional maximal capacity tests were conducted at the end of 2 and 4 weeks of training to account for increases in performance and adjustment of exercise speed during training sessions. As a result, treadmill speed was set to 18cm/s for weeks 1-2, 25.5cm/s for weeks 3-4 and 29cm/s for weeks 5-6 for both groups.

At the end of 6-weeks training a final maximal capacity test was performed to serve as a post training comparison.

2.4. Body composition analysis (Echo-MRI)

Body composition was assessed by nuclear magnetic resonance (Echo MRI-100 Body Composition Analyzer; Echo Medical Systems, Houston, TX) at ZT13 in the week prior to starting exercise training, after 3 weeks and after 6 weeks of exercise training. Lean and fat mass (grams) are presented as percentage changes over time as well as a percentage of total body weight over time.

2.5. Food intake and cage activity measurements

As described above, mice were single housed to track individual food intake and cage activity. Food and body mass were weighed on a weekly basis to assess changes in food intake relative to body weight. The daily activity of the mice in their home cages were continuously recorded throughout the entire experiment using wireless infrared activity monitoring (Actimetrics, Wilmette, IL, USA) and analysed using ClockLab software 7. Average counts per week were calculated for the 4-weeks prior to training, weeks 1-2, 3-4 and 5-6. The hour during treadmill running ± 30 minutes was excluded from each individual's analysis.

2.6. Tissue collection

Animals were humanely sacrificed following the experiment using isoflurane anaesthesia followed by cervical dislocation performed under red light, 48 hours after the exercise trained mice final maximal capacity test at ZT13. Hindlimb muscles and liver were dissected and cleaned of excess fat and connective tissue. Muscles from the left hindlimb were weighed and flash frozen in liquid nitrogen and muscles from the right hindlimb embedded in optimal cutting temperature compound (OCT) before snap freezing in isopentane pre-cooled by liquid nitrogen. Muscles were stored at -80°C until biochemical analysis or cryo-sectioning.

2.7. Blood/serum collection and analysis

Blood samples were collected from the tail veins of all mice at ZT13, 48 hours prior to tissue collection. Blood glucose levels were measured at this point using the OneTouch® UltraMini system (OneTouch Solutions, UK). A whole blood aliquot was kept on ice for assessment of glycosylated haemoglobin content (Hba1c%) (#80310, Crystal Chem High Performance Assays, IL, USA) as per manufacturer's instructions. Endpoint colorimetric measurements were made using the Molecular Devices Spectramax i3X system (Molecular Devices LLC, CA, USA). The remaining blood was collected in EDTA coated serum tubes before centrifugation at 4°C for 10 mins at 2000RCF. Serum was frozen and stored at -20°C. Insulin concentration was measured using a commercially available kit (#90080, Crystal Chem High Performance Assays, IL, USA) as per manufacturer's instructions.

2.8. Gastrocnemius muscle and liver glycogen content analysis

Small (~15mg) snap-frozen pieces from the gastrocnemius muscle and liver (*n*=5 per group) were used to detect glycogen content. Care was taken to ensure the same location of each tissue was sampled across replicates. Tissue samples were weighed and homogenized in 100µl of glycogen hydrolysis buffer in a bullet blender (BBY24M, Next Advance, NY, USA), at speed 10 for two, 2-min sets, at 4°C using 0.5mm stainless steel beads. Homogenates were boiled at 95°C for 5 mins to inactivate enzymes, then centrifuged at 12,000 rpm for 5 mins at 4°C to remove insoluble material. Muscle glycogen concentrations were then quantified from the supernatant using a commercially available kit (Sigma-Aldrich-MAK016) according to manufacturer's instructions. Glycogen concentrations were normalized to input tissue weight.

2.9. Gastrocnemius muscle and liver triglyceride content analysis

Small (~15mg) snap-frozen pieces from the gastrocnemius muscle and liver (*n*=5 per group) were used to detect glycogen content. Care was taken to ensure the same location of each tissue was sampled across replicates. Tissue pieces were weighed and homogenized as above (Section 2.8) in chloroform: methanol (2:1). Samples were incubated for 30 mins at 20°C with shaking at 1,400rpm. Samples were then centrifuged at 13,000rpm for 30 mins at 20°C. The liquid phase was mixed with 0.9% NaCl and centrifuged at 2,000rpm for 5 mins. Chloroform: Triton X-100 (1:1) was added to the organic phase and solvents evaporated. Triglycerides were then measured using a commercially available kit (Abcam, (ab65336), according to manufacturer's instructions. Triglyceride concentrations were normalized to input tissue weight.

2.10. Fibre morphology analysis

Histological samples were transversely sectioned (10µm thick) from the mid-belly of the gastrocnemius, soleus and plantaris muscles and labelled with a cocktail of antibodies against isotype-specific anti-mouse primary antibodies for types IIA (SC-71) and IIB (BF-F3) (1:100) from Developmental Studies Hybridoma Bank (DSHB) (Iowa City, Iowa, USA), and an antibody against dystrophin (1:100, ab15277, Abcam, St. Louis, MO, USA) overnight as previously described [31,32]. Following overnight incubation, sections were washed for 3x5 mins with phosphate buffered saline (PBS) before AlexaFluor secondary antibodies against Rabbit IgG H&L, Mouse IgG1, Mouse IgG2B (Invitrogen/Thermofisher, USA) were added for 2 hours before 3x5 min washes with PBS. Sections were post-fixed in methanol for 5 mins before 3x5 min washes with PBS. Sections were carefully dried to remove excess PBS before mounting in Vectashield Antifade Mounting Medium (Vector Laboratories, UK). For nuclei counting, sections were just labelled with dystrophin and counterstained for nuclei with DAPI. Additional labelling was performed as above using an antibody against embryonic myosin (BF-G6, DSHB). Embryonic myosin positive fibers were counted manually using Image Jv1.53, excluding intrafusal muscle fibers of muscle spindles, and expressed as a percentage of total fibers identified. Manual counting of central nuclei was also performed in this manner. Whole labelled cross sections were imaged at 20x using a Leica TCS SPE microscope equipped with a

DFC7000 camera (Leica, Germany). LAS Navigator software was used to generate a merged image of the whole muscle cross-section. Fiber type distribution, overall muscle fibre cross-sectional area (CSA) and total nuclei/myonuclei per fiber was characterised using MyoVision 2.2 automated software [31]. For succinate dehydrogenase staining, cryosections were incubated at 37°C for 1 hour with a sodium succinate buffer (50mM sodium succinate, 50mM phosphate buffer and 0.5mg/ml nitroblue tetrazolium) before washing in distilled water and imaged as above. Colorimetric images were converted to greyscale 8-bit image and SDH labelling intensity quantified using the polygon selection tool to select within the muscle cross-section and raw intensity density measurement tool as standard in Image Jv1.53.

2.11. Protein extraction, SDS page and western blotting

Gastrocnemius muscles were homogenised as above (Section 2.8) previously described in homogenisation Buffer (10 mM HEPES, pH 7.5, 10 mM MgCl2, 60 mM KCl, 300 mM Sucrose, 0.1 mM EDTA, and complete mini protease inhibitor (Millipore; Cat. #11836170001). Protein concentrations were determined via BCA assay and protein concentration normalised across samples, before resuspension in 4x Laemlli buffer, and heating at 55°C. 10 micrograms of protein were loaded per lane and separated by SDS page using a 4-20% gradient gel. After electrophoresis, gels were semi-dry transferred to nitrocellulose membranes. Equal protein loading was confirmed by total protein staining using (Revert™ 700 Total Protein Stain, Li-COR biosciences, USA). Membranes were washed and subsequently blocked in Tris-buffered saline with 5% non-fat dry milk. A primary antibody cocktail (OxPhos Rodent WB Antibody (45-8099), Thermofisher Scientific, USA)) which contains clones against NDUFB8, SDHB, MTCO1, UQCRC2 and ATP5A was incubated with the membrane overnight at 1:1000. Blots were probed with HRP-conjugated anti-mouse secondary antibody (1:10,000, Thermofisher Scientific, USA) for 1 hour at room temperature. Pierce™ ECL Western Blotting Substrate (Thermofisher Scientific) was used for detection. Images were acquired using Chemidoc Imaging systems (BioRad) and proteins quantified and normalized to total protein content within Image Lab Software (Biorad).

2.12. LC-MS Metabolomics

Gastrocnemius muscle samples (*n* =5 per group) underwent cellular extraction procedures (Southeast Center for Integrated Metabolomics, SECIM). Global metabolomics profiling was performed on a Thermo Q-Exactive Orbitrap mass spectrometer with Dionex UHPLC and autosampler. All samples were normalized by total protein content prior to extraction. Samples were analyzed in positive and negative heated electrospray ionization with a mass resolution of 35,000 at m/z 200 as separate injections. Separation was achieved on an ACE 18-pfp 100 x 2.1 mm, 2 µm column with mobile phase A as 0.1% formic acid in water and mobile phase B as acetonitrile. This is a polar embedded stationary phase that provides comprehensive coverage but does have some

limitations in coverage of very polar species. The flow rate was 350 µL/min with a column temperature of 25°C. 4µL was injected for negative ions and 2 µL for positive ions.

MZmine (freeware) was used to identify features, deisotope, and align features. All adducts and complexes were identified and removed from the data set. The mass and retention time data was searched against SECIMs internal metabolite library, and known metabolites were mapped to KEGG IDs. Blank feature filtering was performed using inner-quartile range filtering as implemented in the R package MetaboAnalystR (https://github.com/xia-lab/MetaboAnalystR). Missing data were imputed by k-nearest neighbour imputation and peak intensities were normalized sample-wise using sum normalization followed by $\log^{10}$ transformation and pareto scaling as implemented R package MetaboAnalystR. Univariate ANOVA was performed using the R package stats (R Core Team 2023) to determine whether there was a significant effect of variable Class on metabolite peak intensity, and post-hoc pairwise comparisons were performed using least-squares means method as implemented in the R package emmeans (R.V. Lenth 2023). Adjusted p-values are adjusted for multiple pairwise comparison testing, not testing of multiple metabolites. A significance threshold was set at an FDR of 5%. Metaboanalyst 5.0[33] was used to perform enrichment analysis on annotated features against the KEGG metabolite set library.

2.13. RNA isolation, library preparation & RNA-sequencing (RNA-seq)

Around 200mg of powdered whole gastrocnemius muscle (inclusive of both medial and lateral heads) (*n* =5 per group) was placed in 1ml of Trizol (Invitrogen, 15596018). Tissue samples were homogenised as above. Homogenates were incubated at room temperature for 5 minutes, mixed with chloroform, and centrifuged at 10,000 rpm for 15 minutes at 4ºC. Following centrifugation, the aqueous upper phase was mixed with isopropanol and transferred to a RNeasy mini spin column (Qiagen). RNA was bound to the column by centrifugation and was washed multiple times as per the manufacturer's recommendations. DNA was digested in the column using the RNase-free DNase set (Qiagen). RNA was eluted in nuclease-free water from the column. RNA integrity numbers (RIN) were determined on an Agilent TapeStation 2200 (Agilent, CA, USA). All samples prepared for sequencing had RIN values of at least 8. Libraries were created using Poly-A tail selection using the Illumina mRNA Prep kit (Illumina, Inc. CA, USA) kit and pooled to equal molarities and sequenced on the Novaseq 6000 (Illumina, Inc. CA, USA) S4 2x150bp platform by the University of Florida Interdisciplinary Centre for Biotechnology Research (ICBR).

2.14. Bioinformatics analysis

FastQ files were imported to Partek® Flow® Genomic Analysis Software Partek Inc. (Missouri, USA) for pipeline processing. Pre-alignment QA/QC was performed on all reads prior to read trimming below a Phred quality score of 25 and adapter trimming. STAR alignment 4.4.1d was used to align reads to the mm10 genome assembly. Aligned reads were then mapped to the Ensembl transcriptome annotation model associated with mm10, release 99_v2. Transcript expression was

normalised using DESeq2 median of ratios and differentially expressed genes (DEGs) identified through the Partek® Flow® DESeq2's binomial generalized linear model, with Wald testing for significance between conditions set at $q < 0.05$. Unless otherwise stated, data is presented as DESeq2 normalized counts with mean ± standard deviation (SD). ~20 million reads where achieved per sample (n=5 per group). Biological interpretation of filtered/selected gene lists was performed in Partek® Flow® Genomic Analysis Software to identify associated Kyoto Encyclopedia of Genes and Genomes (KEGG) pathways. HOMER (v4.11) motif analysis was performed on DEGSs, to identify enrichment of known motifs (6-12bp long) in the gene body and up to 2kb upstream of the transcription start site. QA/QC analysis, alignment, normalized DESeq2 counts, DEG analysis and pathway enrichment analysis can be found within supplementary file 1. Raw RNA-seq data is available at the National Center for Biotechnology Information (NCBI) accession GSE240653.

2.15. Statistical analysis

Unless otherwise stated, physiology data are presented as mean ± standard deviation (SD) and statistical analyses conducted in GraphPad Prism 9.4.1. For multiple comparisons, data were analysed using one, or two factor analysis of variance (ANOVA) followed by Tukey's multiple comparisons test. Repeated measures ANOVA were performed on measures where the same subjects were measured over time. To assess differences between exercise training groups only, two-tailed independent student t-tests were performed to evaluate statistical differences. All statistically significant thresholds were considered at the level of $P < 0.05$. Corresponding symbols to highlight statistical significance are as follows; $*P \leq 0.05$, $**P \leq 0.01$, $***P \leq 0.001$, $****P \leq 0.0001$.

3. Results

3.1. Improvements in exercise performance are not altered by loss of *Bmal1* in skeletal muscle following 6-weeks of training.

We first sought to determine whether loss of skeletal muscle *Bmal1* would affect maximal running capacity in response to progressive, inclined treadmill training. Maximal running performance (measured as work done in arbitrary units) was assessed early in the dark phase, ZT13, in both vehicle-treated and iMSBmal1KO mice before and after 2, 4, and 6 weeks of exercise training which commenced at ~11 months of age, (7-months post tamoxifen treatment), Figure 1A. At baseline, exhaustion speed (cm/s) was significantly higher in the iMSBmal1KO mice than vehicle treated mice, (22 ± 1.3 cm/s vs. 31.6 ± 3.3, $P = 0.0007$). Both vehicle-treated and iMSBmal1KO mice showed a significant increase in exhaustion speed from pre- to post-training ($P < 0.0001$), as depicted in Figure 1B. However, no differences were found between the two groups after 6 weeks of training (52.6 ± 7.8 cm/s vs. 50.8 ± 3.4 cm/s, $P = 0.98$). No differences were observed in maximal work performance between the two groups pre-training, with vehicle-treated mice performing at 1183 ± 239 AU and iMSBmal1KO mice at 1685 ± 524 AU, ($P = 0.35$), (Figure 1C). After 6 weeks of exercise

training, there were no differences in work done between groups in a maximal exercise performance test, with vehicle-treated mice performing at 4710 ± 1106 AU and iMSBmal1KO mice at 4321 ± 552 AU (P = 0.94). However, a significant effect of training status was observed for both groups (P < 0.0001), as shown in Figure 1C. Total work done (AU) across the timecourse of training did not differ between groups and is presented in Supplementary Figure 2A.

Prior to commencement of exercise training no differences in body mass were observed between groups, (Supplementary Figure 2B). Following 6-weeks training there was no significant differences between body mass for both of the exercise trained groups vs. their respective controls (Vehicle: 32.3 ± 2.7g vs. 29.8 ± 0.8g, P = 0.13 and iMSBmal1KO: 34.1 ± 2.5g vs. 30.5 ± 2.4g, P = 0.09) although modest trends were observed, (Figure 1D/Supplementary Figure 2B). Food intake measured per week (g, p/w) per bodyweight (g) did not change over time or between groups across the experimental timecourse, equaling ~0.8-1 times bodyweight per week, (Supplementary Figure 2C). We also note that there were no significant differences between the 4 groups in total activity, dark/active phase activity, or light/inactive phase activity (counts p/w), suggesting that neither loss of *Bmal1* or exercise training affected behavioral cage activity (Supplementary Figure 2D-F).

MRI body composition measurements identified no significant differences in total fat mass, or percentage fat mass as a proportion of total body mass prior to training between vehicle, (3.54 ± 0.53g, 10.4 ± 2.18%) and iMSBmal1KO mice (3.03 ± 0.69g, 9.3 ± 3.2%). However, measurements taken after 3 and 6-weeks of training revealed a progressive decline in total fat mass in both the vehicle exercise trained (pre-training, 3.54 ± 0.53g vs. post-training, 2.4 ± 0.34g, P = 0.0057) and iMSBmal1KO exercise trained mice, (pre-training, 3.03 ± 0.69g vs. post-training, 1.78 ± 0.39g, P = 0.025). There was a significant interaction effect of training on the percent change in fat mass (P = 0.001), but no genotype effect (P = 0.53) was present, (Figure 1E). No genotype (P = 0.052) or training effects were observed with the proportion of fat mass relative to total body weight, (P = 0.1), Figure 1F. Progressive reductions in lean mass (g) were also observed between vehicle exercise trained (pre-training, 26.74 ± 0.86g vs. post-training 25.45 ± 0.65g, P = 0.01), equivalent to a 4.8 ± 1.7% reduction in lean mass. A similar percent reduction (4.98 ± 6.1% reduction) was observed in iMSBmal1KO exercise trained mice (Figure 1G), but this was not statistically significant (pre-training, 26.92 ± 1.62g vs. post-training, 25.52 ± 0.98g, P = 0.07), (Figure 1G), however there was no genotype specific effect (P = 0.9). The proportion of lean mass as a percent of total body mass showed no differences with training (P = 0.17), or genotype (P = 0.15), Figure 1H.

Histological phenotyping was performed on cross-sections of the gastrocnemius muscle, and we found no differences in the main measures of muscle phenotype between genotypes or following exercise training, Supplementary Figure 3A. We highlight that there were no significant differences in muscle weight, fiber cross-sectional area, myonuclei per fiber cross-section or proportion of fiber

types with either muscle specific *Bmal1* knockout, or exercise training (Supplementary Figure 3B-E). We observed similar increases in SDH staining intensity after exercise training but there was no effect on genotype. However, we did notice a small but statistically significant increase in central nuclei (0.92 ± 0.86% fibers vs. 3.9 ± 1.7% fibers, $P < 0.001$) and embryonic positive fibers (0.16 ± 0.13% fibers vs. 1.76 ± 0.84% fibers, $P < 0.001$) after exercise training in the *Bmal1* knockout, which was not present in the vehicle treated group after exercise training, (Supplementary Figure 3G-H).

INSERT FIGURE 1

3.2. Exercise training does not rescue the hyperinsulinemia of muscle specific *Bmal1* knockout mice and blunts increases in glycogen storage.

Exercise is a well-known approach to improve glucose tolerance through increasing skeletal muscle insulin sensitivity and therefore increasing glucose uptake. We hypothesized that exercise training would improve the defective glucose uptake in the iMSBmal1KO muscle independent of the muscle circadian clock, due to promotion of glucose uptake and transport, therefore reducing resting blood glucose and decreasing serum insulin levels. One measure of glucose homeostasis is glycosylated hemoglobin (e.g., Hba1c%), and consistent with our prior data, we found that levels were significantly higher in the iMSBmal1KO control mice vs. vehicle control mice (5.3 ± 0.7% vs. 4.04 ± 10.4%, $P = 0.034$). Levels were lower post exercise training in both groups (vehicle control = 2.38 ± 0.98%, $P = 0.005$, iMSBmal1KO control = 3.38 ± 0.42%, $P = 0.001$), with no differences detected between genotypes of the trained mice, ($P = 0.118$), Figure 2A. Analysis of non-fasted blood glucose in the morning (ZT13, early active phase) was significantly reduced following exercise training in the vehicle treated mice (168.4 ± 6.7mg/dL vs. 139.8 ± 10.4mg/dL, $P = 0.0001$) and was reduced to a similar level in the iMSBmal1KO mouse (169.6 ± 8.6mg/dL vs. 153.2 ± 5mg/dL, $P = 0.0227$), (Figure 2B).

As depicted in Figure 2C, ZT13 non-fasted insulin levels were significantly higher in the control iMSBmal1KO mice, compared with vehicle control mice (0.80 ± 0.07 vs. 0.4 ± 0.08ng/ml, $P < 0.0001$) consistent with prior studies. Levels were reduced following exercise training in both vehicle (0.24 ± 0.06ng/ml, $P = 0.024$) and iMSBmal1KO mice (0.57 ± 0.1ng/ml, $P = 0.0017$) however the levels in the trained iMSBmal1KO mice were still significantly higher than vehicle control (~41%, $P = 0.0196$) and post-training vehicle treated mice (~135%, $P <0.0001$).

Assessments of gastrocnemius glycogen content at ZT13 showed significantly higher levels in the iMSBmal1KO muscles vs vehicle controls (0.51 ± 0.01µg/mg vs. 0.87 ± 0.05µg/mg, $P = 0.034$), Figure 2D, as previously reported [9]. With training, muscle glycogen content increased in both the vehicle to 1.85 ± 0.13µg/mg ($P < 0.0001$) and to 1.43 ± 0.31µg/mg ($P = 0.0006$) in the iMSBmal1KO. However, the vehicle trained muscle achieved a larger increase (262.8% vs. 66.5%) with a higher

concentration of muscle glycogen in comparison to the iMSBmal1KO trained mice, (P = 0.008). Triglyceride content of gastrocnemius muscles was significantly lower at baseline in the iMSBmal1KO control mice in comparison to vehicle treated control mice (0.8 ± 0.17nmol/mg vs. 0.42 ± 0.09nmol/mg, P = 0.0011). Exercise training had no effect in the vehicle (0.88 ± 0.14nmol/mg, P = 0.76) and iMSBmal1KO mice (0.58 ± 0.09 nmol/mg, P = 0.23) respectively relative to their sedentary controls, Figure 2E. Triglyceride content therefore remained significantly lower post-training in the iMSBmal1KO exercise trained mice in comparison to vehicle exercise trained mice, P = 0.0086).

In the liver, glycogen concentrations were ~40% lower in the iMSBmal1KO in comparison to vehicle treated control controls, (9.59 ± 1.86µg/mg vs. 5.48 ± 0.74µg/mg, P < 0.004). Exercise training significantly increased glycogen content in the vehicle-treated liver (16.28 ± 1.81µg/mg, P < 0.0001) and in the iMSBmal1KO liver (13.26 ± 1.64µg/mg, P < 0.0001). Glycogen content was significantly lower in the trained iMSBmal1KO liver in comparison to vehicle trained mice (P = 0.036), Figure 2F. Exercise did not alter triglyceride content of liver in either group, but there were genotype specific effects with iMSBmal1KO control livers having significantly lower levels in comparison to their vehicle counterparts, (1.71 ± 0.18nmol/mg vs. 0.98 ± 0.19nmol/mg, P = 0.0006), Figure 2G.

INSERT FIGURE 2

3.3. Loss of skeletal muscle BMAL1 alters core clock factor gene expression and disrupts the transcriptional regulation of metabolism.

To address the molecular pathways of muscle exercise adaptation in the absence of the clock we performed RNA-seq on gastrocnemius muscle 48 hours after their last exercise bout to query changes in steady state gene expression. As a start we identified 1217 differentially expressed genes (DEGs; q < 0.05) between the sedentary control vs. sedentary iMSBmal1 KO mice; 535 that were upregulated and 682 that were downregulated with muscle specific *Bmal1* knockout respectively. As seen in the volcano plot (Supplementary Figure 4A) and consistent with prior studies[5,8,9,28], many of the clock output genes, such as *Dbp*, *Ppargc1a (Pgc1a)*, *Mylk4*, and *Tcap* were significantly down-regulated[34,35]. Motif analysis of the promoters of the 682 down-regulated genes determined that there was significant enrichment for E-boxes, and these include several circadian clock (CLOCK, NPAS2) specific E-boxes, as well as MYC specific E-box sequences. Other represented motifs in the down-regulated genes include MEF2 or MADS elements and sites for NFAT which are well recognized pathways in skeletal muscle, (Supplementary Figure 4B). Subsequent KEGG pathway functional analysis of the DEGs confirmed significant dysregulation of genes associated with ‘circadian rhythms’ (14 genes), as well as a large number of pathways relating to substrate

metabolism, (Supplementary Figure 4C). Within this pathway, we identified dysregulation of transcripts essential for glucose and glycogen homeostasis including (*Hk2*, *Rab10*, *Slc2a3*, *Slc2a4*, *Tbc1d1*, *Aldoc*, *Fbp2*, *Gbe1*, *Pgm1*, *Pgm2*, *Phka1*, *Pygm*) which is as previously reported and is consistent with the metabolic phenotype that we characterize in Figure 2.

3.4. Identification of clock-dependent and clock-independent transcriptional adaptation to 6-weeks of exercise training.

The observation that mice lacking BMAL1 in skeletal muscle were able to improve exercise performance to similar levels as vehicle treated mice suggested that the molecular adaptations to exercise training would be similar between the muscles. We performed transcriptomic analysis of the gastrocnemius muscle of the control and exercise trained mice, with and without BMAL1. Analysis of the muscle from vehicle control and trained mice identified 142 DEGs after training which is consistent with prior studies [3,36]. Within those DEGs, 67 were upregulated, and 75 were downregulated after training, Figure 3A. Enrichment of DNA binding motifs within the promoter or gene body of the small number of upregulated DEGs included MEF2C, SIX1, Androgen receptor (AR) half sites and NFAT, the latter of which is transcriptionally activated by calcineurin, a Ca^{2+}-dependent phosphatase known to increase after exercise in response to increased Ca^{2+}, (Figure 3B). Downregulated DEGs were enriched for DNA binding motifs relating to NFAT, EGR1 and SMAD4 transcription factors. Pathway analysis revealed that these DEGs were associated with 'PPAR signaling' (11 genes), 'protein digestion and absorption' (8 genes), 'fatty acid metabolism/degradation' (7 genes), 'ECM-receptor interactions' (7 genes), 'focal adhesion' (5 genes), 'calcium signaling' (7 genes), 'PI3K-Akt signaling' (5 genes) and 'HIF-1 signalling' (5 genes), Figure 3C. A number of these DEGs included fatty acid metabolism regulators (*Hadha, Hadhb, Acaa2, Cpt2, Acsl1, Scd2, Acadm, Cd36, Fabp1, Apoa1 and Apoa2*) and these have been well characterised in response to exercise training.

Analysis of the iMSBmal1 KO sedentary and trained mice identified a much larger number of DEGs in the KO muscle following training. A total of 780 DEGs were identified, of which 283 were downregulated and 497 upregulated with exercise training, Figure 3D. There was little overlap of common motifs enriched within the DEGs responsive to exercise training in the iMSBmal1KO mice and vehicle treated mice. This is suggestive of a completely different transcriptional reprogramming occurring in response to training. Analysis of motifs in the downregulated DEGs, found XBP1 sites which is a transcription factor that functions as a regulator of the unfolded protein response and part of the ER stress pathway, (Figure 3E), which was not significantly enriched in the vehicle exercise trained mice. Within the genes upregulated by exercise training in the iMSBmal1KO mouse, motif enrichment analysis included transcription factors sites such as YY1, ESRRA/B, SP1, NRF/1, SMAD2/4 and P53. While many of these represent transcription factors normally associated with an

acute response to exercise (e.g., ESRRA, NRF1, P53) they are not commonly identified as motifs enriched in steady state changes in gene expression[37–42], (Figure 3E). ESRRA is also known to promote aerobic transformation and increase metabolic fuel efficiency in skeletal muscle, as well as enhances lactate clearance by augmenting its oxidation to pyruvate. We also found that the pathways enriched in these muscles were different compared to the vehicle training response. There was a strong enrichment for categories of metabolic reprogramming in the iMSBmal1KO mouse which included the differential expression of 58 genes associated with 'Oxidative Phosphorylation', 122 genes associated with 'Metabolic Pathways', and 12 genes associated with the 'TGF-beta signaling pathway', (Figure 3F). These observations suggest that transcriptional homeostasis is altered following 6 weeks of run training in the muscle without *Bmal1*.

We sought to quantitatively compare the number of common 'exercise-training responsive' genes and found only 23 common factors (1.6% of DEGs) between the training responses using an FDR cut-off of $q = 0.05$. Utilizing a less stringent significance cut-off of $P = 0.01$ revealed only 63 overlapping genes (2.99%) illustrating the large discordance in the transcriptional responses in skeletal muscle associated with improved exercise performance, (Figure 3G). We probed these 63 genes to see if the training responses were directionally similar between the two genotypes, Figure 3H. We determined that 25 (39.7%) genes were commonly upregulated in both genotypes, 6 (9.5%) were commonly downregulated. We identify these as clock independent exercise training genes. Interestingly, 22 (34.9%) genes mainly associated with the extracellular matrix (*Col3a1, Col4a1, Col5a2, Tnxb, Emilin2, Fn1, Lama2, Nid1* and *Nid2*) as well as genes involved in insulin regulation (*Pappa* and *Irs2*) were upregulated in the vehicle but downregulated in the iMSBmal1KO in response to training. We also identified 10 genes (15.9%) including *Coq10a, Cyc1* and *Esrra* that where downregulated with training in the vehicle but were upregulated in the iMSBmal1KO, (Figure 3H). Thus, while they are shared between the two genotypes, the fact that over 50% of the 63 shared genes are regulated in the opposite direction suggests they are exercise responsive, but the directionality is modulated by the presence of absence of BMAL1.

We also asked the question, does exercise training rescue expression of any genes that are dysregulated in iMSBmal1KO muscles. Of the 1216 genes differentially expressed with loss of *Bmal1* in the muscle of sedentary mice, only 94 (7.7%) of these were also differentially expressed in the iMSBmal1KO with exercise training. A heatmap for all 94 genes is presented in Supplemental Figure 6. To address whether exercise training functioned to restore the gene expression in the iMSBmal1KO muscle toward levels seen in the vehicle control muscle we plotted Log^2 fold changes of these genes and calculated Pearson's correlation coefficient, (Figure 3I). Instead of an expected positive correlation, if the exercise had restored normal gene expression, we found a negative correlation ($R^2 = 0.2486$). This outcome indicates that exercise training did not alleviate or rescue the dysregulated gene expression of the majority of these 94 genes, and largely functioned to exacerbate the transcriptional disruption associated with loss of *Bmal1*.

Lastly, we focused analysis on key sets of genes, linked to glucose metabolism and to core clock function, to ask if there were similarities or differences with exercise training between genotypes. We assessed the expression of genes which are essential for glucose and glycogen homeostasis including *Hk2*, *Rab10*, *Slc2a3*, *Slc2a4*, *Tbc1d1*, *Aldoc*, *Fbp2*, *Gbe1*, *Pgm1*, *Pgm2*, *Phka1*, and *Pygm*, Figure 3J. As visualized in the heatmap, there were little to no significant changes in gene expression in the muscle lacking BMAL1. In contrast there were many changes in gene expression in the vehicle trained mice with large increases in *Hk2*, *Hk1* and *Pgm2* and downregulation of *Pgm1*, *Slc2a4* (Glut4) and *Phka1* (Phosphorylase Kinase Regulatory Subunit Alpha 1). A common pattern was seen in the core clock genes with little to no changes in expression of their expression following training in the iMSBmal1KO muscle, but several genes changed in the vehicle exercise training response. Examples include upregulation of *Nfil3*, *Per1* and *Cry2* and down-regulation of *Per3* and *Dbp*. These observations suggest that in order for exercise to alter the expression of genes critical for glucose homeostasis in muscle, BMAL1 and/or a functional clock mechanism are indispensable. Plots with individual data points are provided within supplemental Figure 5.

INSERT FIGURE 3

3.5. Upregulation of mitochondrial gene expression but no change in mitochondrial complex protein abundance is a feature of iMSBmal1KO exercise adaptation.

We next focused on the analysis of the unique DEGs in the trained iMSBmal1KO muscle (Figure 3F). A number of these genes are shared across pathways relating to pyruvate metabolism, the tricarboxylic acid cycle (TCA cycle), fatty acid β-oxidation and genes relating to mitochondrial complex constituents and their associated mitochondrial ribosomal subunits, a schematic of which is provided in Figure 4A along with notations associated with the regulatory genes presented in Figure 4B-C. Within these pathways, we identified that the majority of genes were upregulated in response to exercise training in the iMSBmal1KO mice, whereas vehicle treated mice showed smaller, or no effect at all in response to exercise training.

We observed that key pyruvate transporters of the outer mitochondrial membrane (*Vdac1*) and the inner mitochondrial membrane (*Mpc1*, *Mpc2*) are significantly downregulated by loss of *Bmal1* in skeletal muscle. Previous chromatin immunoprecipitation with sequencing data has identified BMAL1:CLOCK shared binding sites within the promoter regions, suggesting potential transcriptional role for these genes in skeletal muscle[43]. While the expression of glucose metabolism genes was not rescued, we observed partial rescue of a small proportion of ‘pyruvate metabolism and pyruvate dehydrogenase complex’ genes that are dysregulated with loss of BMAL1 in skeletal muscle, (Figure 4B). For example, *Mpc1* and *Vdac1*, gene expression was partially rescued

(from ~61% to ~73% and ~63% to ~80% of vehicle control) but remained significantly lower than vehicle controls. *Mpc2*, the more abundant pyruvate carrier in skeletal muscle was fully rescued and increased to around 15% above vehicle control levels. Genes encoding the pyruvate dehydrogenase complex (*Pdha, Pdhb, Pdhx*) which convert pyruvate to acetyl-CoA and lactate dehydrogenase proteins (*Ldha, Ldhb*) (converting lactate to pyruvate and vice versa) were also significantly upregulated in the iMSBmal1KO mouse with exercise training, a pattern that was not detected in the muscle of vehicle treated mice with exercise training.

Most strikingly in the iMSBmal1KO training response was the robust up-regulation across almost all genes relating to the TCA cycle, β-oxidation and both nuclear and mitochondrially encoded genes within the mitochondria, (Figure 4B-C). Interestingly, 12 genes (*Acaa2, Aco2, Crat, Cs, Dlst, Fh1, Idh3a, Idh3b, Idh3g, Ogdh, Suclg1 and Suclg2*) encoding proteins involved in TCA cycle intermediate and anaplerotic reactions were significantly upregulated in the iMSBmal1KO mouse in response to exercise training, whereas they were downregulated with training in the vehicle. This trend was also observed in a large family of genes associated with Acyl-CoA hydrolysis to fatty acids and coenzyme A and β-oxidation (*Acadl, Acadm, Acads, Acadv1, Acat1, Acot7)* and the trifunctional protein (*Hadh, Hadha, Hadhb*), indicating a response to increased requirements for the use of fatty acids for energy metabolism, Figure 4B. Genes involved in triglyceride biosynthesis were mainly unchanged with exercise training in the iMSBmal1KO.

We also observed upregulation of a large network of both nuclear and mitochondrial encoded genes that were largely unique to the iMSBmal1KO training adaptation. These related to mitochondrial complexes I (n=44), II (n=4), III (n=11), IV (n=15), V (n=18), as well as 22 nuclear and mitochondrial encoded genes related specifically to the large and small mitochondrial ribosomal subunits, (Figure 4C). The majority of these genes were significantly upregulated relative to both vehicle control and vehicle exercise trained mice, as well as iMSBmal1KO control mice. This is consistent with the observation of *Esrra, Esrrb, Nrf/1* and *p53* binding sites that were enriched in these up-regulated genes. However, western blot analysis of ATP5A, UQCRC2, MTCO1, SDHB and NDUFB8 which are commonly used as protein markers of complex I-V showed no significant differences between any group, illustrating a disconnect between mRNA abundance (Figure 4C) and protein abundance (Figure 4D-E). Whether this infers a post-transcriptional issue, issue with translation, or perhaps greater mitochondrial protein turnover in the muscle-specific knockout with exercise training is yet to be established.

INSERT FIGURE 4

3.5. Exacerbated amino acid availability, further depletion of TCA cycle intermediates and indicators of inefficient energy status with exercise training in the iMSBmal1KO mouse.

We next performed untargeted metabolomics to compare potential relationships between metabolite levels associated with transcriptional reprogramming in the iMSBmal1KO with exercise training. Comparing vehicle controls to iMSBmal1KO mice, we found 46 differentially abundant metabolites, (Figure 5A), a comparison that has previously been reported [8,9,12]. Our results confirm similar findings with increased abundance of many free amino acids and disruption of metabolites related to TCA cycle intermediates as evidenced by Metaboanalyst KEGG pathway analysis (Supplementary File 2). Venn diagram analysis showed that there was little overlap of the metabolites changing within the comparisons (Vehicle Control vs. iMSBmal1KO Control; Vehicle Control vs. Vehicle Exercise Trained; iMSBmal1KO Control vs. iMSBmal1KO Exercise Trained). Following exercise training in the vehicle treated mice, we observed only 19 differentially abundant metabolites, whereas we identified 116 in the iMSBmal1KO. We identified only 8 common metabolites in the exercise training response between genotypes which showed enrichment relating to lysine degradation and glutathione metabolism pathways, (Figure 5B).

As metabolome responses to exercise training in murine models have been well documented [19,22,44–47], for the purpose of this study we focused on identifying the metabolite response to exercise training in the iMSBmal1KO mouse and asked if exercise training restored the metabolite phenotype to be more aligned with the vehicle treated mice. Pathway enrichment of the 116 differentially abundant metabolites in the iMSBmal1KO gastrocnemius muscle following exercise training revealed enrichment of metabolites associated with ‘Tyrosine metabolism’, ‘Alanine, aspartate and glutamate metabolism’, ‘Pyruvate metabolism’, along with pathways associated with the TCA cycle and free amino acids, (Figure 5C).

As previously reported[12], elevated amino acid levels make up a significant component of the altered metabolites with loss of skeletal muscle BMAL1. Following exercise training in the iMSBmal1KO, we identified several patterns in the alteration of amino acid abundance, (Figure 5D-F). Levels of threonine and leucine, which can be converted to acetyl-CoA and acetoacetate, are both elevated in the iMSBmal1KO but were both reduced in abundance with exercise training. Aromatic amino acids, tryptophan, phenylalanine and tyrosine which can be metabolized into fumarate and acetoacetate showed a similar relationship, both being elevated in the iMSBmal1KO but reduced with exercise training, (P <0.0001). Interestingly, fumarate is significantly upregulated with loss of BMAL1 in skeletal muscle (P = 0.009), yet 6 weeks of exercise training reduced the metabolites abundance to lower than vehicle controls (P = 0.0019), (Figure 5 E/G). In contrast, malate levels were

not different between vehicle controls and iMSBmal1KO controls, (P = 0.55), but were significantly more abundant after exercise training in the iMSBmal1KO mice, (P = 0.04). In the vehicle exercise trained mice, malate shows the opposite response and is significantly reduced compared with control levels, (P = 0.013) which demonstrates evidence of genotype specific metabolomic effects.

Levels of valine, which contributes carbon molecules to the TCA cycle as succinyl-CoA, were reduced following exercise training to levels similar to vehicle controls. In contrast, glycine, proline, alanine, glutamic acid, asparagine and aspartic acid remained unchanged, or their levels moved further away from vehicle control levels with exercise training in the iMSBmal1KO mouse. Glutamine and histidine which contribute to the TCA cycle through conversion to □-ketoglutarate and methionine, which is eventually converted to succinyl-CoA, showed opposing effects with exercise training between the two genotypes, decreasing in abundance in the vehicle, while increasing in abundance in the iMSBmal1KO. We were surprised that despite our samples being taken 48 hours after their last exercise bout, pyruvate levels were significantly lower by ~180% (P =0.0029) in the iMSBmal1KO mice with exercise training (Figure 5G). This finding falls in line with our transcriptome analysis, that the genes encoding the enzymes required for glucose transport and metabolism are not rescued with exercise training, so pyruvate supplies stay limited. However, there is a compensatory increase in genes involved in pyruvate metabolism and TCA cycle components likely contributing to the diminished steady state levels of pyruvate with training. Despite the reduction in pyruvate, acetyl-CoA levels were significantly increased in the iMSBmal1KO mice after exercise training, (P = 0.024), suggesting that substrates other than pyruvate are contributing to the increase in acetyl-CoA levels, or that the rate of pyruvate conversion is elevated, coupled with lower amounts leading to pyruvate reduction.

Metabolites relating to anaerobic energy systems were also altered with exercise training in the iMSBmal1KO mouse but remained largely unchanged in vehicle treated mice. This included creatine, which is significantly upregulated with loss of BMAL1 (P =0.043) but was restored back to levels similar to vehicle controls with exercise training. Guanidinoacetate, also known as glycocyamine, is the immediate precursor of creatine, synthesized when guanidinoacetate is methylated using S-adenosyl methionine and was significantly upregulated with loss of BMAL1, (P < 0.0001) but was unaffected by exercise training (Figure 5 E/G). We highlight that *Gamt*, the gene which encodes the protein guanidinoacetate N-methyltransferase was ~127% higher than vehicle controls, ~102% higher than vehicle exercise trained muscles and ~55% higher than iMSBmal1KO controls, suggesting an increased demand to generate creatine for energy production in the iMSBmal1KO following exercise training. We also observed a significant increase in creatine phosphate and deoxycarnitine with exercise training in comparison to all other conditions in the

iMSBmal1KO mice, ($P < 0.05$). A summary of amino acids and TCA cycle intermediates affected by exercise training in the iMSBmal1KO is provided in Figure 5H.

INSERT FIGURE 5

4. Discussion

In this investigation, we addressed the contribution of the core circadian clock factor, *Bmal1*, in skeletal muscle to steady state exercise training adaptations in male mice. We determined that mice lacking BMAL1 specifically in skeletal muscle do have the capacity to increase exercise performance over a 6-week training program. However, our multi-omic analyses identified that the adaptive responses of the transcriptome and metabolome in the absence of skeletal muscle *Bmal1* were largely different. This included the observation that exercise training is not sufficient to rescue the dysregulation of genes essential for carbohydrate metabolism in the *Bmal1* knock out skeletal muscles. These results identified a novel circadian clock-dependent program of gene expression in skeletal muscle in response to chronic exercise training. The findings provide important insights into how a functional circadian clock mechanism, necessary for muscle homeostasis, contributes to skeletal muscle remodelling in response to exercise training [4,8,9,12].

The key finding of this study was that the transcriptional reprogramming to exercise training in skeletal muscle was vastly different between mice with and without the core clock gene, BMAL1. We noted that although the treadmill performances were the same, the adaptation of the transcriptome after exercise training required a quantitatively larger reprogramming with very few genes in common (~2%) resulting in different enriched pathways and putative upstream transcriptional networks between the vehicle and iMSBmal1KO mice. It is important to note that of the subset of common exercise responsive genes between the mouse models (n=63), only half of them change in the same direction. These outcomes suggest that the well-defined molecular responses to exercise training in skeletal muscle requires BMAL1 and/or a functional circadian clock mechanism, but in its absence requires a far larger network of genes to elicit adaptations. Our findings have similarities to recent work demonstrating the contribution of muscle specific *Ppargc1a* to the exercise training response [36]. This is not surprising as it has been shown that *Ppargc1a* is a clock output gene in skeletal muscle. The muscle from skeletal muscle *Ppargc1a* KO mice showed divergent transcriptional responses to training with a shared training response of 32% between the two genotypes. While similar, we detected an shared training response of only 2% between wildtype and muscle specific BMAL1 KO muscle. This suggests that exercise training works with the circadian clock either directly or in collaboration with clock output genes, such as *Ppargc1a*, to regulate the molecular adaptations to exercise training [36].

Pre-clinical and clinical studies have demonstrated the efficacy of both acute and exercise training interventions for improving glucose tolerance and insulin sensitivity in a variety of metabolic

conditions and disorders [48–53]. Our data suggests that exercise training is not sufficient to restore normal insulin sensitivity (as evidenced by continued high insulin levels) in the absence of skeletal muscle BMAL1. While we did detect partial improvement in systemic glucose levels, we suggest these improvements were linked more to the global exercise benefits in other non-muscle tissues such as liver[54–56]. This conclusion is supported by patterns and pathways of gene expression related to glucose transport and metabolism in skeletal muscle that are dysregulated in the absence of BMAL1 and remain dysregulated after exercise training[9,12,43]. Alongside metabolic disorders, recent work has demonstrated the fundamental importance of BMAL1 in different organ systems for the maintenance of physiological homeostasis. Recent results from cardiac *Bmal1* knockout mice have demonstrated that cardiac dysfunction caused by loss of BMAL1 cannot be attenuated with a similar exercise training paradigm[57]. Furthermore, BMAL1 and a functional circadian programme has been shown to be important in order to exert the gero- and neuro-protective effects of exercise, as well as decreasing vulnerability to infectious injury[58]. These findings implicate a functional and aligned circadian clock mechanism across peripheral tissues is fundamental for maintaining metabolic homeostasis and systemic health [59–63].

Our metabolomic analysis provided evidence that exercise training results in different metabolic perturbations to skeletal muscle that are still present 48-hours after their last exercise bout in iMSBmal1KO mice. This suggests that exercise training results in an adaptation to a homeostatic set point that differs from their vehicle treated counterparts. These changes occurred despite the mice achieving similar exercise training workloads and performance capacities. Our results are suggestive of continued low glycolytic flux and upregulation of pathways required for TCA cycle anaplerosis and oxidative phosphorylation with exercise training. Consistent with these observations, we identified that both the nuclear and mitochondrial transcriptomes likely act to compensate for the metabolic dysregulation and mitochondrial disruption[12,29] in the iMSBmal1KO muscle with the extensive upregulation of TCA cycle enzymes and transporters, as well as oxidative phosphorylation/ mitochondrial components.

In conclusion, our investigation has uncovered the importance of skeletal muscle BMAL1, likely through circadian clock function, for directing skeletal muscle adaptation to exercise training. Our analysis defined clock dependent and non-clock dependent transcriptional adaptations to exercise. Specifically, we highlight the importance of BMAL1 in the transcriptional regulation of energy metabolism given that our results show BMAL1 is seemingly indispensable for the regulation of glucose metabolism genes which cannot be rescued by exercise training. With loss of skeletal muscle BMAL1, exercise training alters the basal homeostasis of muscle through a divergent transcriptional exercise adaptation programme with differential metabolomic outcomes.

Acknowledgements

We would like to thank Dr. Daniel Kopinke at the University of Florida for the use of his microscope. We also extend our thanks to the Gene Expression & Genotyping (GE) core, RRID:SCR_019145, and NextGen DNA Sequencing (NS) core, RRID:SCR_019152 and the Southeast Center for Integrated Metabolomics, (SECIM) at the University of Florida for library preparation, DNA sequencing and metabolomics respectively. This work was supported by NIH R01AR079220 to KAE.

References

[1] Amar, D., Gay, N.R., Beltran, P.M.J., Adkins, J.N., Armenteros, J.J.A., Ashley, E., et al., 2022. Temporal dynamics of the multi-omic response to endurance exercise training across tissues. bioRxiv.

[2] Egan, B., Sharples, A.P., 2022. Molecular Responses to Acute Exercise and Their Relevance for Adaptations in Skeletal Muscle to Exercise Training. Physiological Reviews.

[3] Viggars, M.R., Sutherland, H., Lanmüller, H., Schmoll, M., Bijak, M., Jarvis, J.C., 2023. Adaptation of the transcriptional response to resistance exercise over 4 weeks of daily training. The FASEB Journal 37(1): e22686, Doi: 10.1096/fj.202201418R.

[4] Dyar, K.A., Ciciliot, S., Wright, L.E., Biensø, R.S., Tagliazucchi, G.M., Patel, V.R., et al., 2014. Muscle insulin sensitivity and glucose metabolism are controlled by the intrinsic muscle clock. Molecular Metabolism 3(1): 29–41, Doi: 10.1016/j.molmet.2013.10.005.

[5] Schroder, E.A., Harfmann, B.D., Zhang, X., Srikuea, R., England, J.H., Hodge, B.A., et al., 2015. Intrinsic muscle clock is necessary for musculoskeletal health. The Journal of Physiology 593(24): 5387–404.

[6] Ripperger, J.A., Schibler, U., 2006. Rhythmic CLOCK-BMAL1 binding to multiple E-box motifs drives circadian Dbp transcription and chromatin transitions. Nature Genetics 38(3): 369–74, Doi: 10.1038/ng1738.

[7] Menet, J.S., Pescatore, S., Rosbash, M., 2014. CLOCK:BMAL1 is a pioneer-like transcription factor. Genes & Development 28(1): 8–13, Doi: 10.1101/gad.228536.113.

[8] Hodge, B.A., Wen, Y., Riley, L.A., Zhang, X., England, J.H., Harfmann, B.D., et al., 2015. The endogenous molecular clock orchestrates the temporal separation of substrate metabolism in skeletal muscle. Skeletal Muscle 5(1): 1–16.

[9] Harfmann, B.D., Schroder, E.A., Kachman, M.T., Hodge, B.A., Zhang, X., Esser, K.A., 2016. Muscle-specific loss of Bmal1 leads to disrupted tissue glucose metabolism and systemic glucose homeostasis. Skeletal Muscle 6(1): 12, Doi: 10.1186/s13395-016-0082-x.

[10] Zitting, K.-M., Vujovic, N., Yuan, R.K., Isherwood, C.M., Medina, J.E., Wang, W., et al., 2018. Human resting energy expenditure varies with circadian phase. Current Biology 28(22): 3685-3690. e3.

[11] Wolff, C.A., Gutierrez-Monreal, M.A., Meng, L., Zhang, X., Douma, L.G., Costello, H.M., et al., 2022. Defining the age-dependent and tissue-specific circadian transcriptome in male mice. Genomics.

[12] Dyar, K.A., Hubert, M.J., Mir, A.A., Ciciliot, S., Lutter, D., Greulich, F., et al., 2018. Transcriptional programming of lipid and amino acid metabolism by the skeletal muscle circadian clock. PLOS Biology 16(8): e2005886, Doi: 10.1371/journal.pbio.2005886.

[13] Akashi, M., Tsuchiya, Y., Yoshino, T., Nishida, E., 2002. Control of Intracellular Dynamics of Mammalian Period Proteins by Casein Kinase I ε (CKIε) and CKI□ in Cultured Cells. MOL. CELL. BIOL. 22: 11.

[14] Camacho, F., Cilio, M., Guo, Y., Virshup, D.M., Patel, K., Khorkova, O., et al., 2001. Human casein kinase Iδ phosphorylation of human circadian clock proteins period 1 and 2. FEBS Letters 489(2–3): 159–65, Doi: 10.1016/S0014-5793(00)02434-0.

[15] Etchegaray, J.-P., Machida, K.K., Noton, E., Constance, C.M., Dallmann, R., Di Napoli, M.N., et al., 2009. Casein Kinase 1 Delta Regulates the Pace of the Mammalian Circadian Clock. Molecular and Cellular Biology 29(14): 3853–66, Doi: 10.1128/MCB.00338-09.

[16] Thomas, J.M., Kern, P.A., Bush, H.M., McQuerry, K.J., Black, W.S., Clasey, J.L., et al., 2020. Circadian rhythm phase shifts caused by timed exercise vary with chronotype. JCI Insight 5(3): e134270, Doi: 10.1172/jci.insight.134270.
[17] Kemler, D., Wolff, C.A., Esser, K.A., 2020. Time-of-day dependent effects of contractile activity on the phase of the skeletal muscle clock. The Journal of Physiology 598(17): 3631–44, Doi: 10.1113/JP279779.
[18] Wolff, C.A., Esser, K.A., 2020. Exercise sets the muscle clock with a calcium assist. The Journal of Physiology 598(24): 5591–2, Doi: 10.1113/JP280783.
[19] Sato, S., Basse, A.L., Schönke, M., Chen, S., Samad, M., Altıntaş, A., et al., 2019. Time of Exercise Specifies the Impact on Muscle Metabolic Pathways and Systemic Energy Homeostasis. Cell Metabolism 30(1): 92-110.e4, Doi: 10.1016/j.cmet.2019.03.013.
[20] Sato, S., Dyar, K.A., Treebak, J.T., Jepsen, S.L., Ehrlich, A.M., Ashcroft, S.P., et al., 2022. Atlas of exercise metabolism reveals time-dependent signatures of metabolic homeostasis. Cell Metabolism 34(2): 329-345.e8, Doi: 10.1016/j.cmet.2021.12.016.
[21] Savikj, M., Gabriel, B.M., Alm, P.S., Smith, J., Caidahl, K., Björnholm, M., et al., 2019. Afternoon exercise is more efficacious than morning exercise at improving blood glucose levels in individuals with type 2 diabetes: a randomised crossover trial. Diabetologia 62(2): 233–7, Doi: 10.1007/s00125-018-4767-z.
[22] Savikj, M., Stocks, B., Sato, S., Caidahl, K., Krook, A., Deshmukh, A.S., et al., 2022. Exercise timing influences multi-tissue metabolome and skeletal muscle proteome profiles in type 2 diabetic patients – A randomized crossover trial. Metabolism 135: 155268, Doi: 10.1016/j.metabol.2022.155268.
[23] Dyar, K.A., Ciciliot, S., Tagliazucchi, G.M., Pallafacchina, G., Tothova, J., Argentini, C., et al., 2015. The calcineurin-NFAT pathway controls activity-dependent circadian gene expression in slow skeletal muscle. Molecular Metabolism 4(11): 823–33.
[24] Casanova-Vallve, N., Duglan, D., Vaughan, M.E., Pariollaud, M., Handzlik, M.K., Fan, W., et al., 2022. Daily running enhances molecular and physiological circadian rhythms in skeletal muscle. Molecular Metabolism 61: 101504, Doi: 10.1016/j.molmet.2022.101504.
[25] Douglas, C.M., Hesketh, S.J., Esser, K.A., 2021. Time of Day and Muscle Strength: A Circadian Output? Physiology 36(1): 44–51, Doi: 10.1152/physiol.00030.2020.
[26] Stuart J. Hesketh, Casey L. Sexton, Christopher A. Wolff, Mark R. Viggars, Karyn A. Esser, 2023. Early morning run-training results in enhanced endurance performance adaptations in mice. bioRxiv: 2023.09.18.557933, Doi: 10.1101/2023.09.18.557933.
[27] Ab Malik, Z., Bowden Davies, K.A., Hall, E.C., Barrett, J., Pullinger, S.A., Erskine, R.M., et al., 2020. Diurnal differences in human muscle isometric force in vivo are associated with differential phosphorylation of sarcomeric M-band proteins. Proteomes 8(3): 22.
[28] Martin, R.A., Viggars, M.R., Esser, K.A., 2023. Metabolism and exercise: the skeletal muscle clock takes centre stage. Nature Reviews Endocrinology: 1–13.
[29] Fernández-Martínez, J., Ramírez-Casas, Y., Aranda-Martínez, P., López-Rodríguez, A., Sayed, R.K.A., Escames, G., et al., n.d. iMS-Bmal1−/− mice show evident signs of sarcopenia that are counteracted by exercise and melatonin therapies. Journal of Pineal Research n/a(n/a): e12912, Doi: 10.1111/jpi.12912.
[30] Avila, J.J., Kim, S.K., Massett, M.P., 2017. Differences in Exercise Capacity and Responses to Training in 24 Inbred Mouse Strains. Frontiers in Physiology 8: 974, Doi: 10.3389/fphys.2017.00974.
[31] Viggars, M.R., Wen, Y., Peterson, C.A., Jarvis, J.C., 2022. Automated cross-sectional analysis of trained, severely atrophied, and recovering rat skeletal muscles using MyoVision 2.0. Journal of Applied Physiology 132(3): 593–610, Doi: 10.1152/japplphysiol.00491.2021.
[32] Murach, K.A., Mobley, C.B., Zdunek, C.J., Frick, K.K., Jones, S.R., McCarthy, J.J., et al., 2020. Muscle memory: myonuclear accretion, maintenance, morphology, and miRNA levels with

811 training and detraining in adult mice. Journal of Cachexia, Sarcopenia and Muscle 11(6): 1705–
812 22, Doi: 10.1002/jcsm.12617.
813 [33] Pang, Z., Zhou, G., Ewald, J., Chang, L., Hacariz, O., Basu, N., et al., 2022. Using MetaboAnalyst
814 5.0 for LC–HRMS spectra processing, multi-omics integration and covariate adjustment of
815 global metabolomics data. Nature Protocols 17(8): 1735–61.
816 [34] Liu, C., Li, S., Liu, T., Borjigin, J., Lin, J.D., 2007. Transcriptional coactivator PGC-1α integrates
817 the mammalian clock and energy metabolism. Nature 447(7143): 477–81.
818 [35] Andrews, J.L., Zhang, X., McCarthy, J.J., McDearmon, E.L., Hornberger, T.A., Russell, B., et al.,
819 2010. CLOCK and BMAL1 regulate MyoD and are necessary for maintenance of skeletal muscle
820 phenotype and function. Proceedings of the National Academy of Sciences 107(44): 19090–5.
821 [36] Furrer, R., Heim, B., Schmid, S., Dilbaz, S., Adak, V., Nordström, K.J.V., et al., 2023. Molecular
822 control of endurance training adaptation in male mouse skeletal muscle. Nature Metabolism,
823 Doi: 10.1038/s42255-023-00891-y.
824 [37] Dings, M.P., van der Zalm, A.P., Bootsma, S., van Maanen, T.F., Waasdorp, C., van den Ende, T.,
825 et al., 2022. Estrogen-related receptor alpha drives mitochondrial biogenesis and resistance to
826 neoadjuvant chemoradiation in esophageal cancer. Cell Reports Medicine 3(11).
827 [38] Tripathi, M., Yen, P.M., Singh, B.K., 2020. Estrogen-related receptor alpha: an under-
828 appreciated potential target for the treatment of metabolic diseases. International Journal of
829 Molecular Sciences 21(5): 1645.
830 [39] Kan, J., Hu, Y., Ge, Y., Zhang, W., Lu, S., Zhao, C., et al., 2021. Declined expressions of vast
831 mitochondria-related genes represented by CYCS and transcription factor ESRRA in skeletal
832 muscle aging. Bioengineered 12(1): 3485–502.
833 [40] Billon, C., Sitaula, S., Banerjee, S., Welch, R., Elgendy, B., Hegazy, L., et al., 2023. Synthetic
834 ERRα/β/γ Agonist Induces an ERRα-Dependent Acute Aerobic Exercise Response and Enhances
835 Exercise Capacity. ACS Chemical Biology 18(4): 756–71.
836 [41] Baar, K., Wende, A.R., Jones, T.E., Marison, M., Nolte, L.A., Chen, M.A.Y., et al., 2002.
837 Adaptations of skeletal muscle to exercise: rapid increase in the transcriptional coactivator
838 PGC-1. The FASEB Journal 16(14): 1879–86.
839 [42] Xia, H., Scholtes, C., Dufour, C.R., Guluzian, C., Giguère, V., 2023. ERRα fosters running
840 endurance by driving myofiber aerobic transformation and fuel efficiency. Molecular
841 Metabolism: 101814, Doi: 10.1016/j.molmet.2023.101814.
842 [43] Gabriel, B.M., Altıntaş, A., Smith, J.A., Sardon-Puig, L., Zhang, X., Basse, A.L., et al., 2021.
843 Disrupted circadian oscillations in type 2 diabetes are linked to altered rhythmic mitochondrial
844 metabolism in skeletal muscle. Science Advances 7(43): eabi9654.
845 [44] Group, M.S., Amar, D., Gay, N.R., Jean Beltran, P.M., Adkins, J.N., Almagro Armenteros, J.J., et
846 al., 2022. Temporal dynamics of the multi-omic response to endurance exercise training across
847 tissues. BioRxiv: 2022.09. 21.508770.
848 [45] Han, S., Wu, Q., Wang, M., Yang, M., Sun, C., Liang, J., et al., 2023. An integrative profiling of
849 metabolome and transcriptome in the plasma and skeletal muscle following an exercise
850 intervention in diet-induced obese mice. Journal of Molecular Cell Biology: mjad016.
851 [46] Hatazawa, Y., Senoo, N., Tadaishi, M., Ogawa, Y., Ezaki, O., Kamei, Y., et al., 2015. Metabolomic
852 analysis of the skeletal muscle of mice overexpressing PGC-1α. PloS One 10(6): e0129084.
853 [47] Pérez-Schindler, J., Kanhere, A., Edwards, L., Allwood, J.W., Dunn, W.B., Schenk, S., et al., 2017.
854 Exercise and high-fat feeding remodel transcript-metabolite interactive networks in mouse
855 skeletal muscle. Scientific Reports 7(1): 13485.
856 [48] Cui, D., Drake, J.C., Wilson, R.J., Shute, R.J., Lewellen, B., Zhang, M., et al., 2020. A novel
857 voluntary weightlifting model in mice promotes muscle adaptation and insulin sensitivity with
858 simultaneous enhancement of autophagy and mTOR pathway. FASEB Journal: Official
859 Publication of the Federation of American Societies for Experimental Biology 34(6): 7330.

[49] Bronczek, G.A., Soares, G.M., de Barros, J.F., Vettorazzi, J.F., Kurauti, M.A., Marconato-Júnior, E., et al., 2021. Resistance exercise training improves glucose homeostasis by enhancing insulin secretion in C57BL/6 mice. Scientific Reports 11(1): 8574.
[50] HOLLOSZY, J.O., SCHULTZ, J., KUSNIERKIEWICZ, J., HAGBERG, J.M., EHSANI, A.A., 1986. Effects of exercise on glucose tolerance and insulin resistance: brief review and some preliminary results. Acta Medica Scandinavica 220(S711): 55–65.
[51] Flockhart, M., Nilsson, L.C., Tais, S., Ekblom, B., Apró, W., Larsen, F.J., 2021. Excessive exercise training causes mitochondrial functional impairment and decreases glucose tolerance in healthy volunteers. Cell Metabolism 33(5): 957-970. e6.
[52] Schneider, S.H., Amorosa, L.F., Khachadurian, A.K., Ruderman, N.B., 1984. Studies on the mechanism of improved glucose control during regular exercise in type 2 (non-insulin-dependent) diabetes. Diabetologia 26: 355–60.
[53] Sylow, L., Kleinert, M., Richter, E.A., Jensen, T.E., 2017. Exercise-stimulated glucose uptake—regulation and implications for glycaemic control. Nature Reviews Endocrinology 13(3): 133–48.
[54] Pederson, B.A., Cope, C.R., Schroeder, J.M., Smith, M.W., Irimia, J.M., Thurberg, B.L., et al., 2005. Exercise capacity of mice genetically lacking muscle glycogen synthase: in mice, muscle glycogen is not essential for exercise. Journal of Biological Chemistry 280(17): 17260–5.
[55] Muoio, D.M., MacLean, P.S., Lang, D.B., Li, S., Houmard, J.A., Way, J.M., et al., 2002. Fatty acid homeostasis and induction of lipid regulatory genes in skeletal muscles of peroxisome proliferator-activated receptor (PPAR) α knock-out mice: evidence for compensatory regulation by PPARδ. Journal of Biological Chemistry 277(29): 26089–97.
[56] Xin, H., Huang, R., Zhou, M., Chen, J., Zhang, J., Zhou, T., et al., 2023. Daytime-restricted feeding enhances running endurance without prior exercise in mice. Nature Metabolism: 1–16.
[57] Yusifova, M., Yusifov, A., Polson, S.M., Todd, W.D., Schmitt, E.E., Bruns, D.R., 2023. Voluntary wheel running exercise does not attenuate circadian and cardiac dysfunction caused by conditional deletion of Bmal1. Journal of Biological Rhythms: 07487304231152398.
[58] Sun, S., Ma, S., Cai, Y., Wang, S., Ren, J., Yang, Y., et al., 2023. A single-cell transcriptomic atlas of exercise-induced anti-inflammatory and geroprotective effects across the body. The Innovation 4(1).
[59] Smith, J.G., Koronowski, K.B., Mortimer, T., Sato, T., Greco, C.M., Petrus, P., et al., 2023. Liver and muscle circadian clocks cooperate to support glucose tolerance in mice. Cell Reports 42(6): 112588, Doi: 10.1016/j.celrep.2023.112588.
[60] Greco, C.M., Koronowski, K.B., Smith, J.G., Shi, J., Kunderfranco, P., Carriero, R., et al., 2021. Integration of feeding behavior by the liver circadian clock reveals network dependency of metabolic rhythms. Science Advances 7(39), Doi: 10.1126/sciadv.abi7828.
[61] Ehlen, J.C., Brager, A.J., Baggs, J., Pinckney, L., Gray, C.L., DeBruyne, J.P., et al., 2017. Bmal1 function in skeletal muscle regulates sleep. Elife 6: e26557.
[62] McDearmon, E.L., Patel, K.N., Ko, C.H., Walisser, J.A., Schook, A.C., Chong, J.L., et al., 2006. Dissecting the functions of the mammalian clock protein BMAL1 by tissue-specific rescue in mice. Science 314(5803): 1304–8.
[63] Smith, J.G., Molendijk, J., Blazev, R., Chen, W.H., Zhang, Q., Litwin, C., et al., 2023. Impact of Bmal1 rescue and time-restricted feeding on liver and muscle proteomes during the active phase in mice. bioRxiv: 2023.06. 12.544652.

Supplemental Files

Supplementary Dataset 1: QA/QC analysis, RNA-seq alignment, normalized DESeq2 counts, DEG analysis and pathway enrichment analysis.

Supplementary Dataset 2: Western Blots, Metabolomic analysis and Metaboanalyst Pathway Analysis.

Figure Legends

Figure 1: Exercise performance, training capacity in vehicle treated and iMSBmal1KO mice. The experimental design is illustrated in (A) which shows the timecourse and parameters of exercise training, physiological testing and tissue collection. At ~4 months of age, iMSBmal1$^{fl/fl}$ were treated with either a vehicle, or vehicle with tamoxifen for 5 days (2mg/day) to induce Cre-recombination and loss of *Bmal1* specifically in skeletal muscle. Both vehicle and iMSBmal1KO mice were randomly assigned to 6 weeks of exercise training performed at ZT13, or control groups. Maximum work done tests were performed prior to, after 2, 4 and 6-weeks of training with the speed adjusted accordingly to make training progressive. MRIs were performed before, after 3 and 6 weeks of training. Mice from all groups were euthanised, and tissue was collected at ZT13, 48 hours after their final maximum work done test. Panel (B/C) shows the results of the maximal exhaustion test, including exhaustion speed (cm/s) and work done (AU). (D) Measurements of body mass were taken before, after 3 and 6 weeks of training and the subsequent percent change calculated for each individual. (E) Total fat mass (g) measured before, after 3 and 6 weeks of training. (F) Percent changes in fat mass (g) were calculated from the beginning of the training period to the middle and end of the training period. (G) Total lean mass (g) measured before, after 3 and 6 weeks of training. (H) Percent changes in lean mass (g) were calculated from the beginning of the training period to the middle and end of the training period.

Figure 2: Metabolic indices of vehicle treated and iMSBmal1KO mice with and without 6-weeks exercise training taken at ZT13. (A) Blood hemoglobin A1C percentage (Hba1c%), (B) resting blood glucose (mg/dL), (C) resting serum insulin (ng/dL), (D) gastrocnemius muscle glycogen concentration (µg/mg), (E) gastrocnemius muscle triglyceride concentration (nmol/mg), (F) liver glycogen concentration (µg/mg), (G) liver triglyceride concentration (nmol/mg). Significance for one way ANOVA analysis is presented as $*P \leq 0.05$, $**P \leq 0.01$, $***P \leq 0.001$, $****P \leq 0.0001$.

Figure 3: iMSBmal1KO gastrocnemius muscles present a larger and divergent transcriptional adaptation to 6-weeks of exercise training. (A) Volcano plot illustrating DEGs between vehicle control and vehicle exercise trained mice. A total of 142 (75 downregulated, 67 upregulated) genes were differentially expressed using an FDR cut off of <0.05. (B) HOMER Motif analysis performed on up and downregulated DEGs identifies a number of transcription factors regulating the transcriptional response to normal exercise adaptation. (C) KEGG Pathway analysis of genes associated with the vehicle treated transcriptional response to exercise training. (D) Volcano plot illustrating DEGs between iMSBmal1KO control and iMSBmal1KO exercise trained mice. A total of

780 (283 downregulated, 497 upregulated) genes were differentially expressed using an FDR cut off of <0.05. (E) HOMER Motif analysis performed on up and downregulated DEGs identifies a number of transcription factors regulating the transcriptional response to exercise adaptation in the absence of skeletal muscle Bmal1. (F) KEGG Pathway analysis of genes associated with the iMSBmal1KO transcriptional remodeling to exercise training. (G) Venn diagram overlapping of DEG responses to vehicle and iMSBmal1KO exercise training at P <0.01 (vehicle response). Minimal overlap in the transcriptional exercise responses is present between vehicle treated and iMSBmal1KO mice using a lenient significance cut off (63 out of 2107, 2.99% overlap). (H) Pie chart of the 63 common exercise training responsive genes in both genotypes reveals common and oppositely regulated gene reprogramming. (I) Analysis of DEGs affected by loss of BMAL1 and exercise training responsive DEGs in the iMSBma1KO mice, reveals 94 common genes. Pearson's correlation of the 94 common DEGs (Log^2 fold changes) reveals that genes affected with Bmal1KO are not rescued with exercise training. (J) Heatmap presenting Log^2 Z-scores for core clock factors/clock output genes and genes associated with glucose handling and glycogen utilisation. Exercise training does not rescue the downregulation of these genes in iMSBmal1KO mice.

Figure 4: Compensatory upregulation of genes associated with pyruvate oxidation, TCA cycle, β-oxidation, mitochondrial complexes and mitoribosome subunits after exercise training in the iMSBmal1KO mouse. (A) Schematic of biological processes involved in providing acetyl-CoA from carbohydrates and lipids for the TCA cycle. Subsequently, the TCA cycle provides NADH and $FADH_2$ for the electron transport chain. Components are numbered/labelled for clarity of the associated genes presented in panels B and C. (B) Heatmaps presenting genes associated with pyruvate oxidation, TCA cycle and β-oxidation, (Log^2 Z-scores). (C) Heatmap presenting genes associated with mitochondrial complexes I-V and the mitochondrial ribosome (Log^2 Z-scores). (D) Western blot of an oxidative phosphorylation antibody cocktail targeting proteins from each mitochondrial complex (NDUFB8, SDHB, UQCR2, MTCO1, ATP5A). (E) Semi-quantitative analysis of mitochondrial complexes. Data is presented as arbitrary units of the densitometry. Significance for one way ANOVA analysis is presented as $*P \leq 0.05$, $**P \leq 0.01$, $***P \leq 0.001$, $****P \leq 0.0001$.

Figure 5: Loss of *Bmal1* in skeletal muscle disrupts the metabolomic rewiring in response to exercise training and causes depletion of TCA cycle intermediates. (A) Table of differentially abundant metabolites ($q < 0.05$) with loss of skeletal muscle BMAL1, the vehicle exercise training response and the iMSBmal1KO exercise training response. (B) Venn diagram analysis of the different comparisons reveals little overlap and divergent metabolomic adaptations to exercise training. (C) Metaboanalyst KEGG metabolite pathway analysis of the iMSBmal1KO exercise training response. Numbers indicate the number of metabolites identified within the pathway. (D) Heatmap illustrating

normalized metabolite abundance for amino acids. (E) Heatmap illustrating normalized metabolite abundance for metabolites relating to glycolysis and the TCA cycle. (F) Boxplots of highlighted amino acids changing with loss of BMAL1 and exercise training. (G) Boxplots of highlighted TCA cycle metabolites/phosphocreatine changing with loss of BMAL1 and exercise training. (H) Summary diagram of TCA cycle metabolites affected with exercise training in the iMSBmal1KO (Blue indicates higher abundance, red indicates lower abundance. Significance for one way ANOVA analysis is presented as $*P \leq 0.05$, $**P \leq 0.01$, $***P \leq 0.001$, $****P \leq 0.0001$.

Supplemental Figure Legends:

Supplemental Figure 1: (A) Confirmation of successful Bmal1 Cre-Recombination in gastrocnemius muscles.

Supplemental Figure 2: Panel (A) illustrates the weekly work done (AU) during exercise training. (B) The amount of food consumed per week was measured and is presented as a proportion of body weight. (C) Measurements of body mass were taken weekly. Habitual cage activity as measured by infrared cage monitors revealed no change in total activity levels between groups. (D) Total Activity. (E) Activity restricted to the dark/active phase. (F) Activity restricted to the light/inactive phase.

Supplemental Figure 3: Histological phenotyping of gastrocnemius muscle. (A) Gastrocnemius muscle wet weight is presented as milligrams per gram of body weight. Myovision 2.0 software was used to automatically assess the average fiber cross-sectional area (μm^2) (B), the proportion of different fiber types (expressed as a percentage of all fibers) (C). (D) Gastrocnemius SDH intensity value (Log10 AU). Myovision 2.0 assessments of the total number of nuclei per fiber cross-section (E), the number of myonuclei per fiber cross-section (F). (G) illustrates the % of fibers with central nuclei and (H) illustrates the % of fibers that were embryonic myosin positive. (I) Representative dystrophin and DAPI images for each respective group. Scale bars indicate 100µm. (J) Representative immunofluorescent images depicting whole cross-section gastrocnemius muscles from each experimental condition labeled with Type IIA/Type IIX/B. Scale bars indicate 1800µm. Data are presented as mean ± standard deviation or min-max values for box plots. Significance for one-way ANOVA analysis is presented as $*P \leq 0.05$, $**P \leq 0.01$, $***P \leq 0.001$.

Supplemental Figure 4: Loss of Bmal1 in skeletal muscle causes transcriptional disruption of circadian rhythms, substrate metabolism and energy sensing pathways. (A) Volcano plot illustrating the DEGs between vehicle control and iMSBmal1KO controls. A total of 1217 (682 downregulated, 535 upregulated) genes were differentially expressed using an FDR cut off of <0.05. (B) HOMER Motif analysis performed on up and downregulated DEGs identifies a number of transcription factors regulating the transcriptional response to loss of Bmal1 in skeletal muscle. (C) KEGG Pathway

analysis reveals disruption of circadian rhythms, metabolic pathways and cell cycle/energy sensing pathways with loss of BMAL1 in skeletal muscle.

Supplemental Figure 5: ZT13 core clock factor gene expression (Deseq2 normalized counts) in the gastrocnemius muscle in response to muscle specific Bmal1KO, exercise training and the combination of the two treatments. Data is presented as mean ± standard deviation. Significance for one way ANOVA analysis is presented as $*P \leq 0.05$, $**P \leq 0.01$, $***P \leq 0.001$, $****P \leq 0.0001$.

Supplemental Figure 6: Heatmap representing the 94 genes overlapping the vehicle control vs. iMSBmal1KO Control statistical comparison and iMSBmal1KO Control vs. iMSBmal1KO exercise trained statistical comparison.

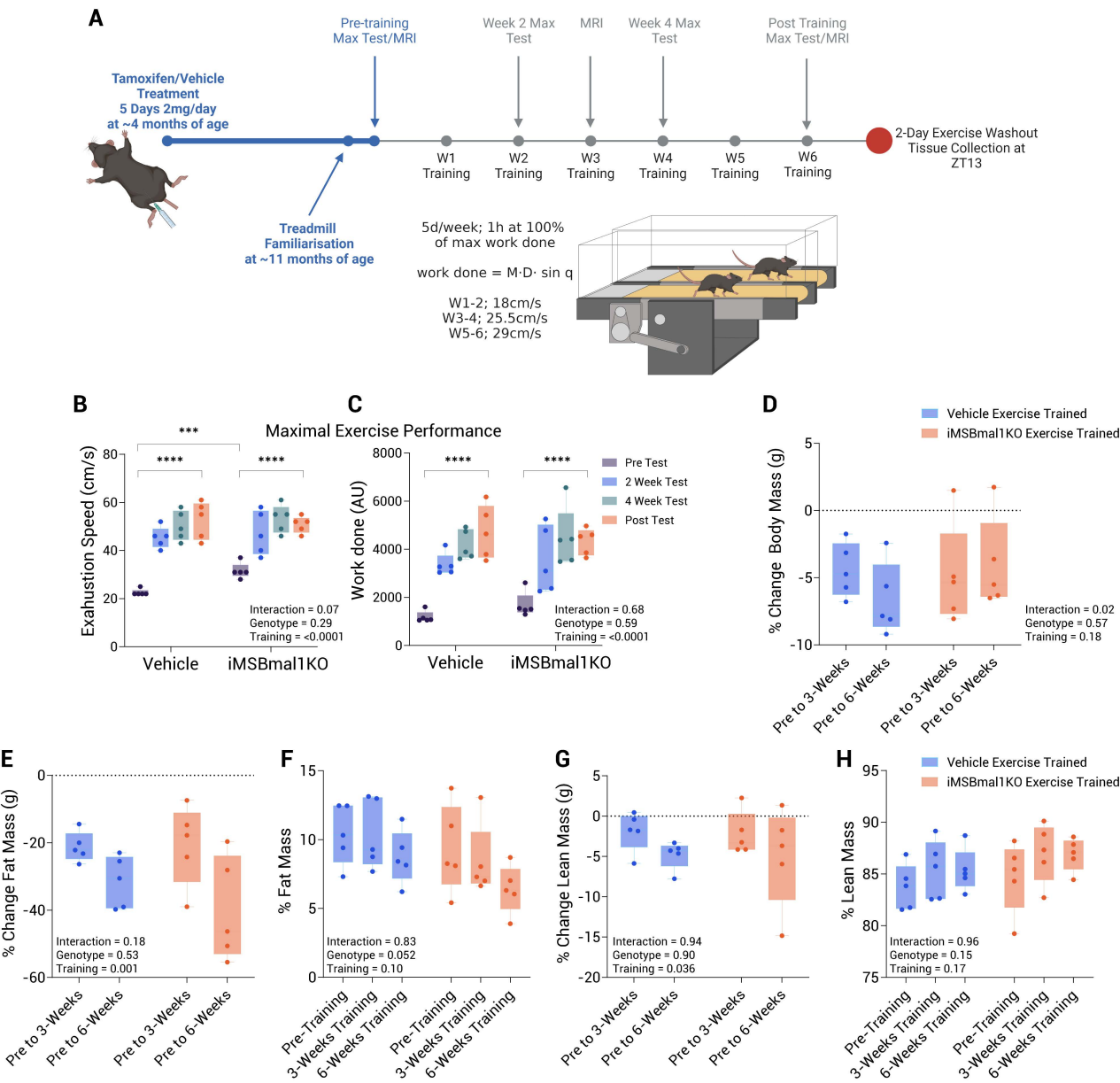
A
Pre-training Max Test/MRI
Week 2 Max Test
MRI
Week 4 Max Test
Post Training Max Test/MRI
Tamoxifen/Vehicle Treatment 5 Days 2mg/day at ~4 months of age
W1 Training
W2 Training
W3 Training
W4 Training
W5 Training
W6 Training
2-Day Exercise Washout Tissue Collection at ZT13
Treadmill Familiarisation at ~11 months of age
5d/week; 1h at 100% of max work done
work done = M·D· sin q
W1-2; 18cm/s
W3-4; 25.5cm/s
W5-6; 29cm/s
B
Exahustion Speed (cm/s)
Interaction = 0.07
Genotype = 0.29
Training = <0.0001
Vehicle
iMSBmal1KO
C
Maximal Exercise Performance
Work done (AU)
Pre Test
2 Week Test
4 Week Test
Post Test
Interaction = 0.68
Genotype = 0.59
Training = <0.0001
D
Vehicle Exercise Trained
iMSBmal1KO Exercise Trained
% Change Body Mass (g)
Interaction = 0.02
Genotype = 0.57
Training = 0.18
Pre to 3-Weeks
Pre to 6-Weeks
E
% Change Fat Mass (g)
Interaction = 0.18
Genotype = 0.53
Training = 0.001
F
% Fat Mass
Interaction = 0.83
Genotype = 0.052
Training = 0.10
Pre-Training
3-Weeks Training
6-Weeks Training
G
% Change Lean Mass (g)
Interaction = 0.94
Genotype = 0.90
Training = 0.036
H
% Lean Mass
Interaction = 0.96
Genotype = 0.15
Training = 0.17

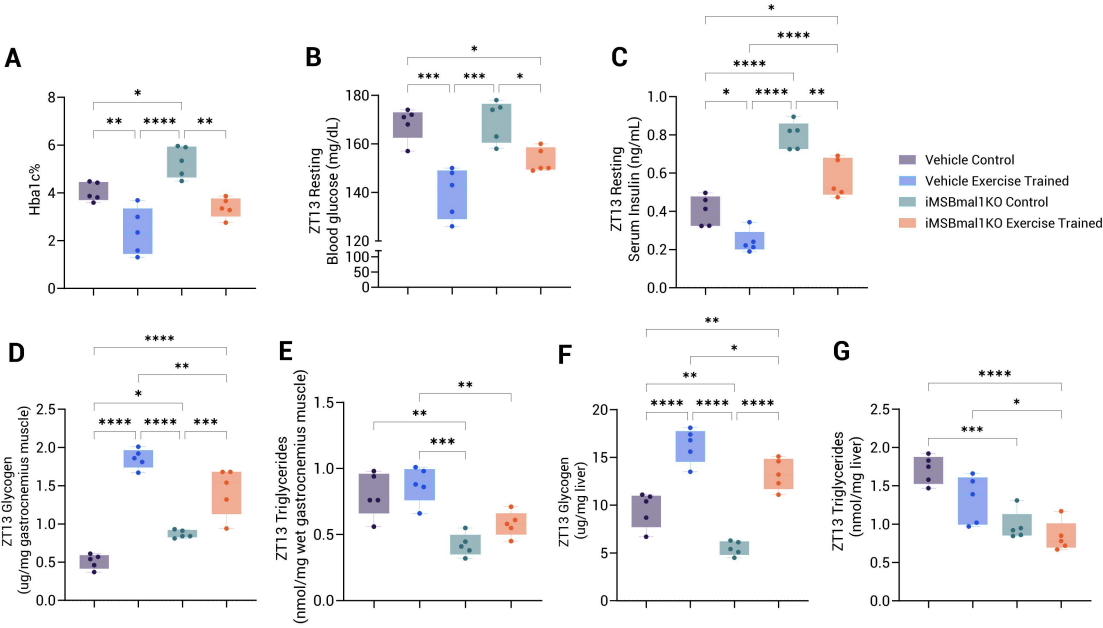
A
Hba1c%
B
ZT13 Resting
Blood glucose (mg/dL)
C
ZT13 Resting
Serum Insulin (ng/mL)
Vehicle Control
Vehicle Exercise Trained
iMSBmal1KO Control
iMSBmal1KO Exercise Trained
D
ZT13 Glycogen
(ug/mg gastrocnemius muscle)
E
ZT13 Triglycerides
(nmol/mg wet gastrocnemius muscle)
F
ZT13 Glycogen
(ug/mg liver)
G
ZT13 Triglycerides
(nmol/mg liver)

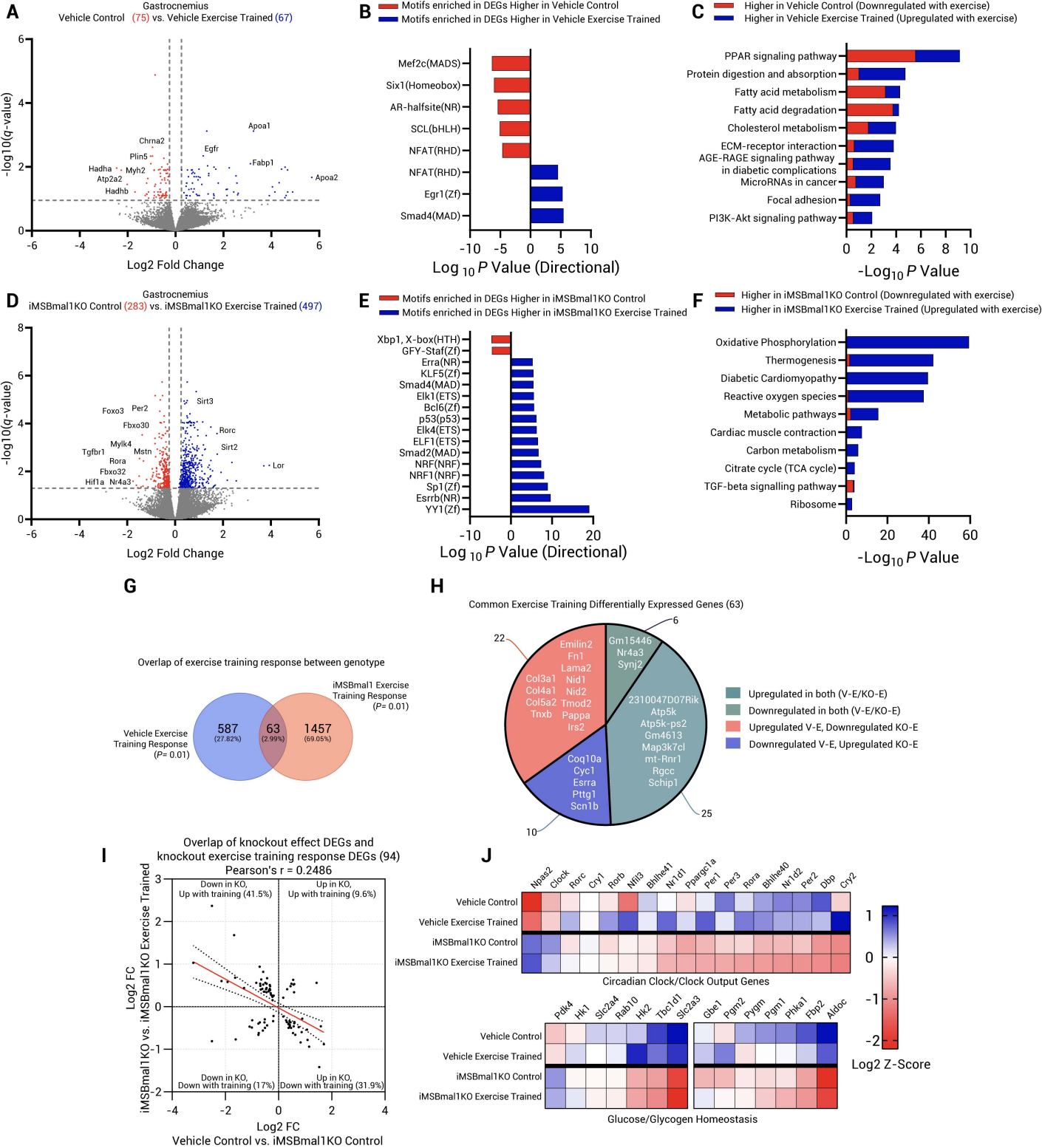
A
Gastrocnemius
Vehicle Control (75) vs. Vehicle Exercise Trained (67)
-log10(q-value)
Log2 Fold Change
Apoa1
Chrna2
Egfr
Plin5
Fabp1
Hadha
Myh2
Atp2a2
Apoa2
Hadhb
B
Motifs enriched in DEGs Higher in Vehicle Control
Motifs enriched in DEGs Higher in Vehicle Exercise Trained
Mef2c(MADS)
Six1(Homeobox)
AR-halfsite(NR)
SCL(bHLH)
NFAT(RHD)
NFAT(RHD)
Egr1(Zf)
Smad4(MAD)
Log 10 P Value (Directional)
C
Higher in Vehicle Control (Downregulated with exercise)
Higher in Vehicle Exercise Trained (Upregulated with exercise)
PPAR signaling pathway
Protein digestion and absorption
Fatty acid metabolism
Fatty acid degradation
Cholesterol metabolism
ECM-receptor interaction
AGE-RAGE signaling pathway in diabetic complications
MicroRNAs in cancer
Focal adhesion
PI3K-Akt signaling pathway
-Log10 P Value
D
Gastrocnemius
iMSBmal1KO Control (283) vs. iMSBmal1KO Exercise Trained (497)
-log10(q-value)
Log2 Fold Change
Sirt3
Foxo3
Per2
Fbxo30
Rorc
Mylk4
Sirt2
Tgfbr1
Mstn
Rora
Lor
Fbxo32
Hif1a
Nr4a3
E
Motifs enriched in DEGs Higher in iMSBmal1KO Control
Motifs enriched in DEGs Higher in iMSBmal1KO Exercise Trained
Xbp1, X-box(HTH)
GFY-Staf(Zf)
Erra(NR)
KLF5(Zf)
Smad4(MAD)
Elk1(ETS)
Bcl6(Zf)
p53(p53)
Elk4(ETS)
ELF1(ETS)
Smad2(MAD)
NRF(NRF)
NRF1(NRF)
Sp1(Zf)
Esrrb(NR)
YY1(Zf)
Log 10 P Value (Directional)
F
Higher in iMSBmal1KO Control (Downregulated with exercise)
Higher in iMSBmal1KO Exercise Trained (Upregulated with exercise)
Oxidative Phosphorylation
Thermogenesis
Diabetic Cardiomyopathy
Reactive oxygen species
Metabolic pathways
Cardiac muscle contraction
Carbon metabolism
Citrate cycle (TCA cycle)
TGF-beta signalling pathway
Ribosome
-Log10 P Value
G
Overlap of exercise training response between genotype
Vehicle Exercise Training Response (P= 0.01)
iMSBmal1 Exercise Training Response (P= 0.01)
587 (27.82%)
63 (2.99%)
1457 (69.05%)
H
Common Exercise Training Differentially Expressed Genes (63)
22
6
25
10
Emilin2 Fn1 Lama2 Nid1 Nid2 Tmod2 Pappa Irs2
Col3a1 Col4a1 Col5a2 Tnxb
Gm15446 Nr4a3 Synj2
2310047D07Rik Atp5k Atp5k-ps2 Gm4613 Map3k7cl mt-Rnr1 Rgcc Schip1
Coq10a Cyc1 Esrra Pttg1 Scn1b
Upregulated in both (V-E/KO-E)
Downregulated in both (V-E/KO-E)
Upregulated V-E, Downregulated KO-E
Downregulated V-E, Upregulated KO-E
I
Overlap of knockout effect DEGs and knockout exercise training response DEGs (94)
Pearson's r = 0.2486
Down in KO, Up with training (41.5%)
Up in KO, Up with training (9.6%)
Down in KO, Down with training (17%)
Up in KO, Down with training (31.9%)
Log2 FC
iMSBmal1KO vs. iMSBmal1KO Exercise Trained
Log2 FC
Vehicle Control vs. iMSBmal1KO Control
J
Npas2 Clock Rorc Cry1 Rorb Nfil3 Bhlhe41 Nr1d1 Ppargc1a Per1 Per3 Rora Bhlhe40 Nr1d2 Per2 Dbp Cry2
Vehicle Control
Vehicle Exercise Trained
iMSBmal1KO Control
iMSBmal1KO Exercise Trained
Circadian Clock/Clock Output Genes
Pdk4 Hk1 Slc2a4 Rab10 Hk2 Tbc1d1 Slc2a3 Gbe1 Pgm2 Pygm Pgm1 Phka1 Fbp2 Aldoc
Vehicle Control
Vehicle Exercise Trained
iMSBmal1KO Control
iMSBmal1KO Exercise Trained
Glucose/Glycogen Homeostasis
Log2 Z-Score

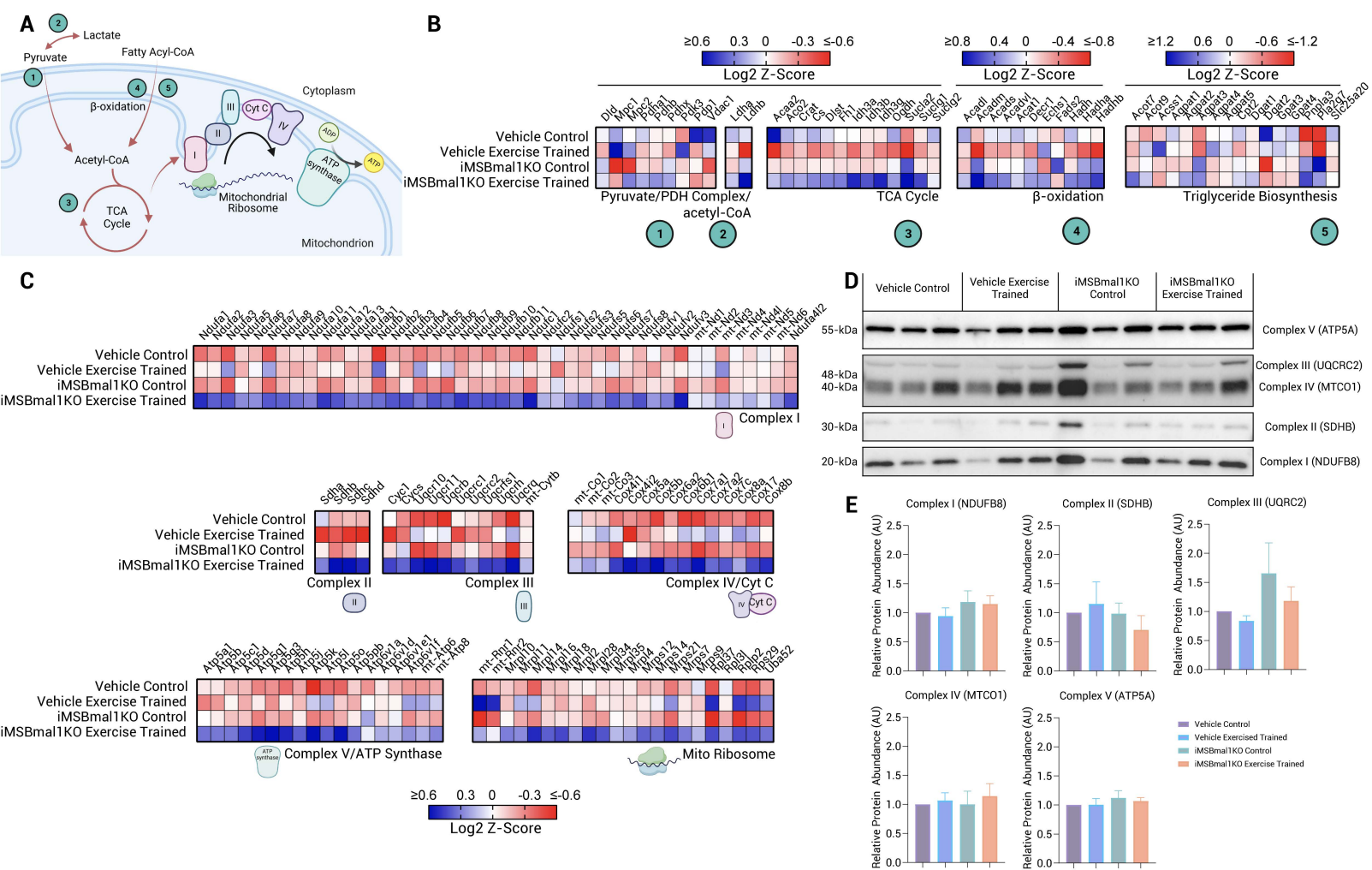
A
Lactate
Pyruvate
Fatty Acyl-CoA
β-oxidation
Cytoplasm
Acetyl-CoA
TCA Cycle
Cyt C
ATP synthase
ADP
ATP
Mitochondrial Ribosome
Mitochondrion
B
Log2 Z-Score
Vehicle Control
Vehicle Exercise Trained
iMSBmal1KO Control
iMSBmal1KO Exercise Trained
Pyruvate/PDH Complex/ acetyl-CoA
TCA Cycle
β-oxidation
Triglyceride Biosynthesis
C
Complex I
Complex II
Complex III
Complex IV/Cyt C
Complex V/ATP Synthase
Mito Ribosome
D
Vehicle Control
Vehicle Exercise Trained
iMSBmal1KO Control
iMSBmal1KO Exercise Trained
55-kDa
48-kDa
40-kDa
30-kDa
20-kDa
Complex V (ATP5A)
Complex III (UQCRC2)
Complex IV (MTCO1)
Complex II (SDHB)
Complex I (NDUFB8)
E
Complex I (NDUFB8)
Complex II (SDHB)
Complex III (UQRC2)
Complex IV (MTCO1)
Complex V (ATP5A)
Relative Protein Abundance (AU)
Vehicle Control
Vehicle Exercised Trained
iMSBmal1KO Control
iMSBmal1KO Exercise Trained

A

Comparison	Number of Altered Metabolites
Vehicle Control vs iMSBmal1KO Control	47
Vehicle Exercise Training Response	19
iMSBmal1KO Exercise Training Response	116

B

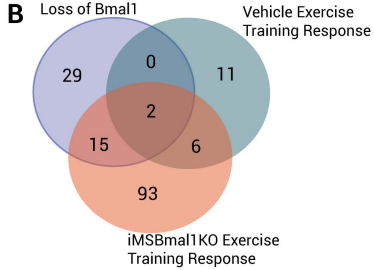

C

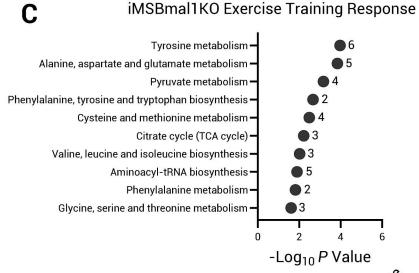

D

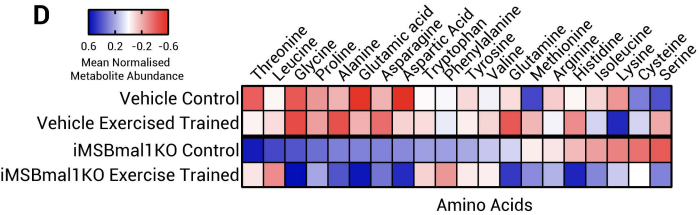

E

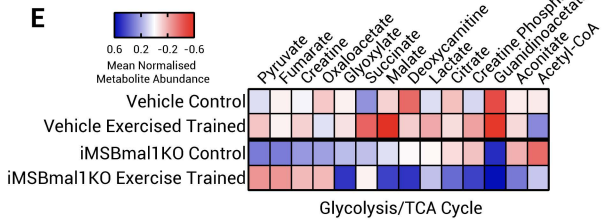

F

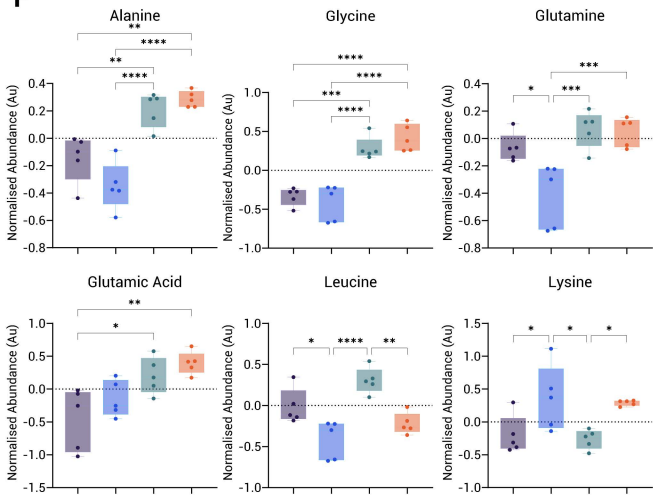

G

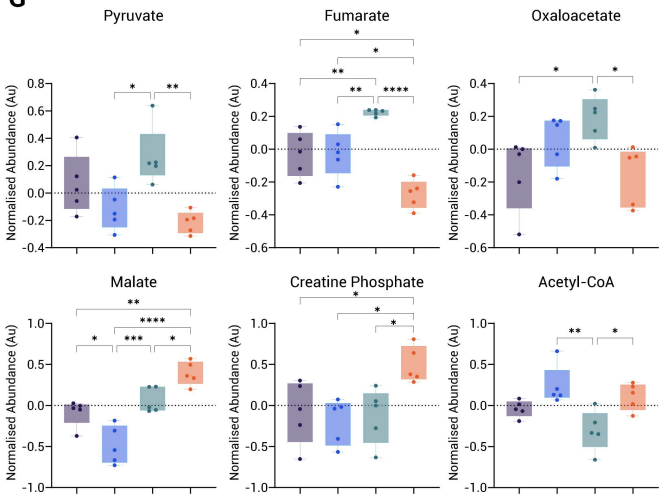

H

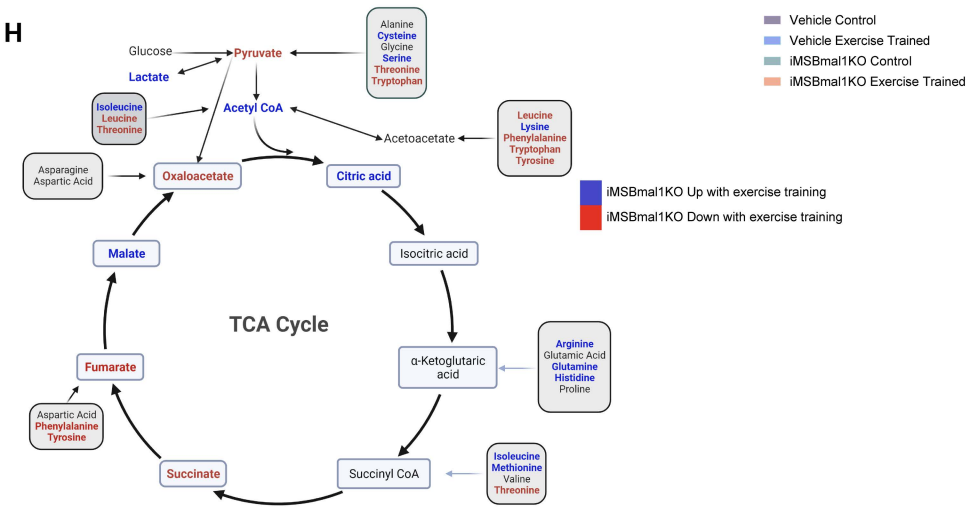

A

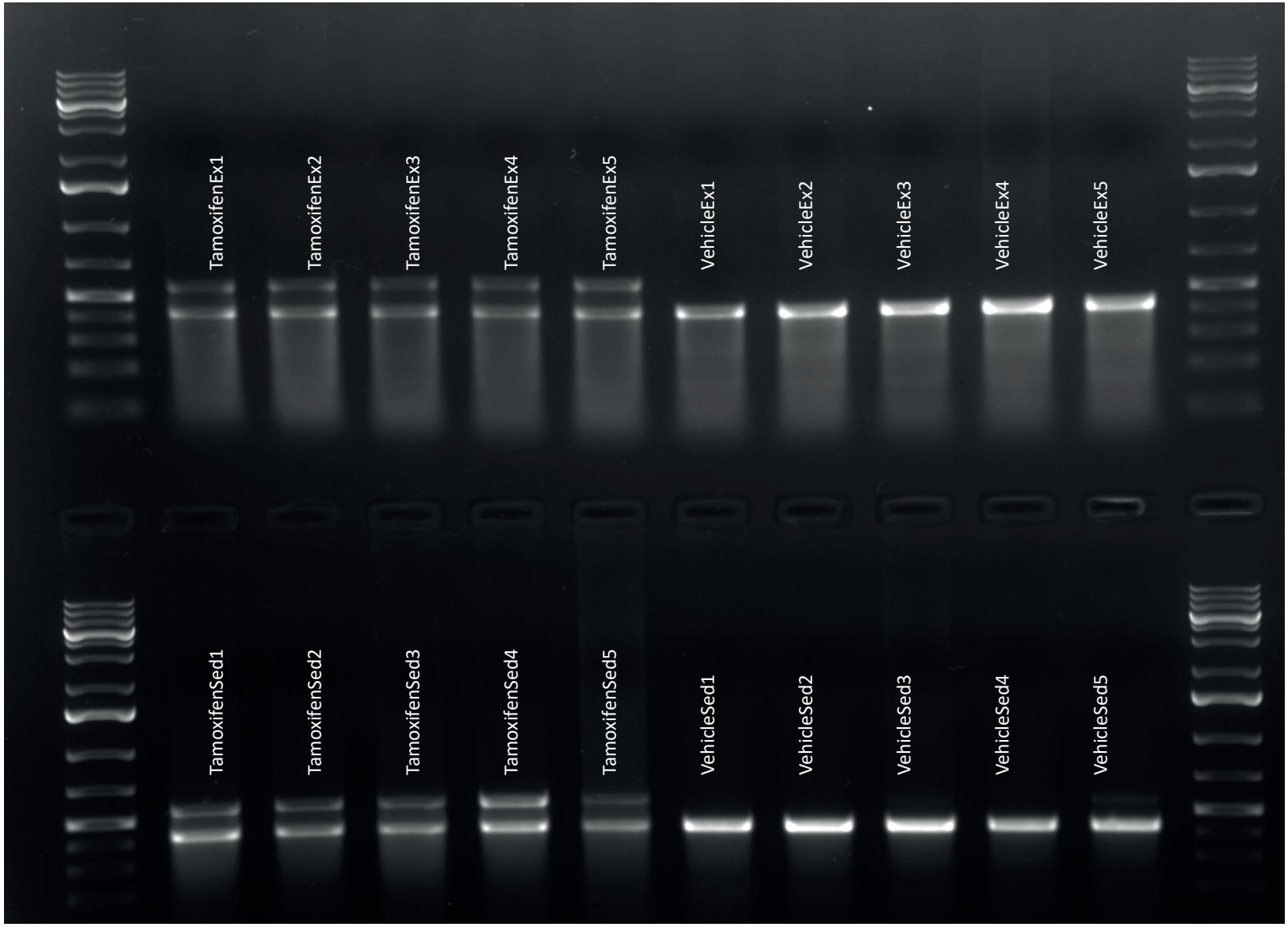
TamoxifenEx1
TamoxifenEx2
TamoxifenEx3
TamoxifenEx4
TamoxifenEx5
VehicleEx1
VehicleEx2
VehicleEx3
VehicleEx4
VehicleEx5
TamoxifenSed1
TamoxifenSed2
TamoxifenSed3
TamoxifenSed4
TamoxifenSed5
VehicleSed1
VehicleSed2
VehicleSed3
VehicleSed4
VehicleSed5

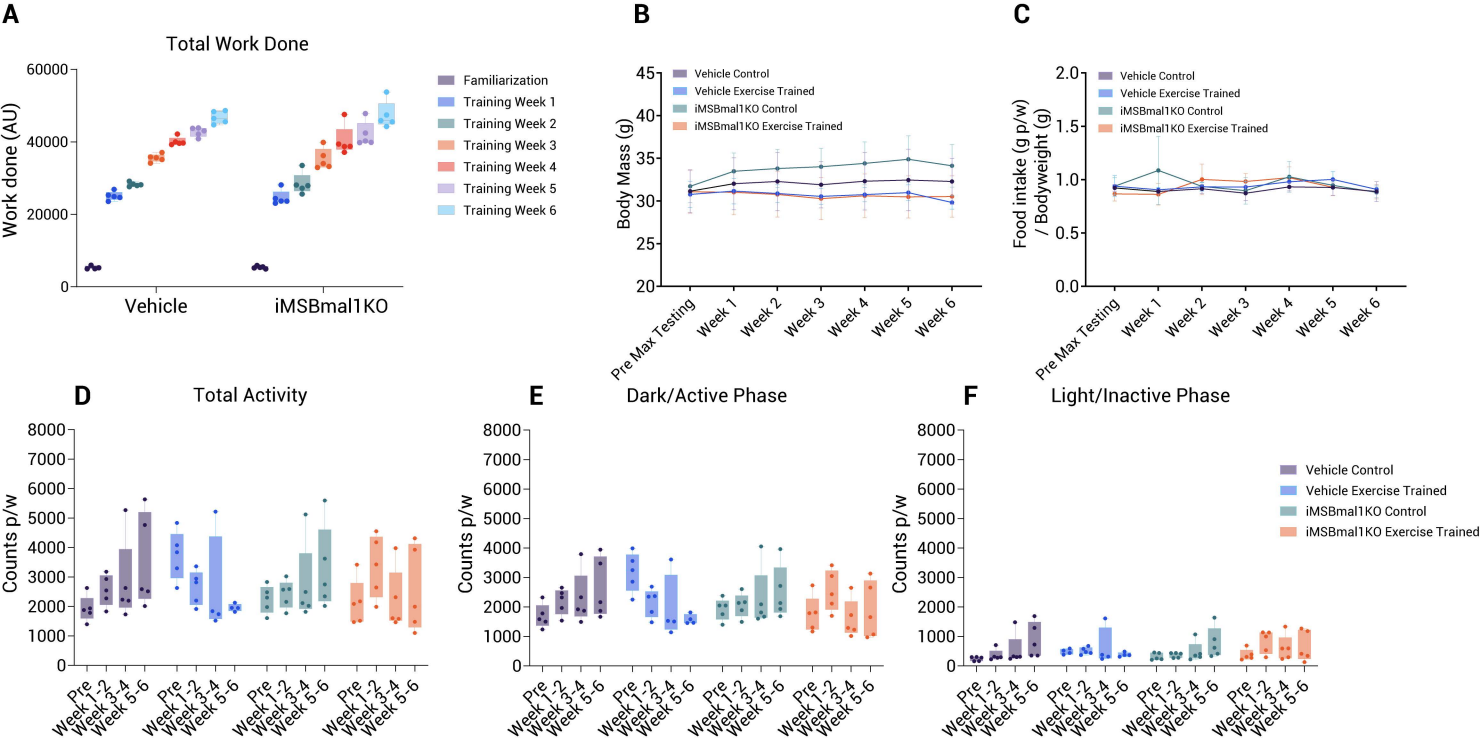
A
Total Work Done
Work done (AU)
60000
40000
20000
0
Vehicle
iMSBmal1KO
Familiarization
Training Week 1
Training Week 2
Training Week 3
Training Week 4
Training Week 5
Training Week 6
B
Body Mass (g)
45
40
35
30
25
20
Vehicle Control
Vehicle Exercise Trained
iMSBmal1KO Control
iMSBmal1KO Exercise Trained
Pre Max Testing
Week 1
Week 2
Week 3
Week 4
Week 5
Week 6
C
Food intake (g p/w) / Bodyweight (g)
2.0
1.5
1.0
0.5
0.0
Vehicle Control
Vehicle Exercise Trained
iMSBmal1KO Control
iMSBmal1KO Exercise Trained
Pre Max Testing
Week 1
Week 2
Week 3
Week 4
Week 5
Week 6
D
Total Activity
Counts p/w
8000
7000
6000
5000
4000
3000
2000
1000
0
Pre
Week 1-2
Week 3-4
Week 5-6
E
Dark/Active Phase
Counts p/w
F
Light/Inactive Phase
Counts p/w
Vehicle Control
Vehicle Exercise Trained
iMSBmal1KO Control
iMSBmal1KO Exercise Trained

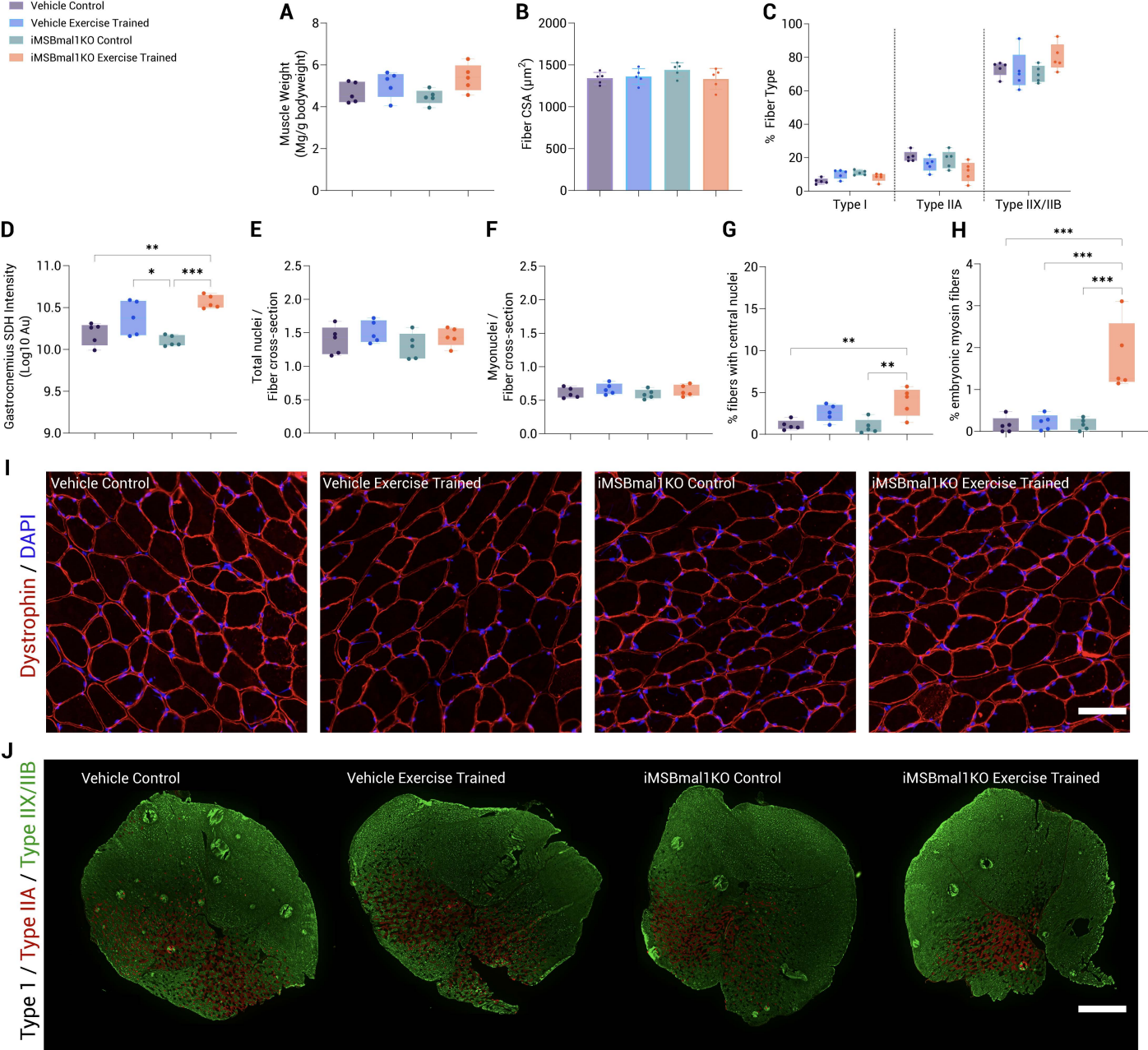
Vehicle Control
Vehicle Exercise Trained
iMSBmal1KO Control
iMSBmal1KO Exercise Trained
A
Muscle Weight (Mg/g bodyweight)
B
Fiber CSA (μm²)
C
% Fiber Type
Type I
Type IIA
Type IIX/IIB
D
Gastrocnemius SDH Intensity (Log10 Au)
E
Total nuclei / Fiber cross-section
F
Myonuclei / Fiber cross-section
G
% fibers with central nuclei
H
% embryonic myosin fibers
I
Dystrophin / DAPI
Vehicle Control
Vehicle Exercise Trained
iMSBmal1KO Control
iMSBmal1KO Exercise Trained
J
Type 1 / Type IIA / Type IIX/IIB
Vehicle Control
Vehicle Exercise Trained
iMSBmal1KO Control
iMSBmal1KO Exercise Trained

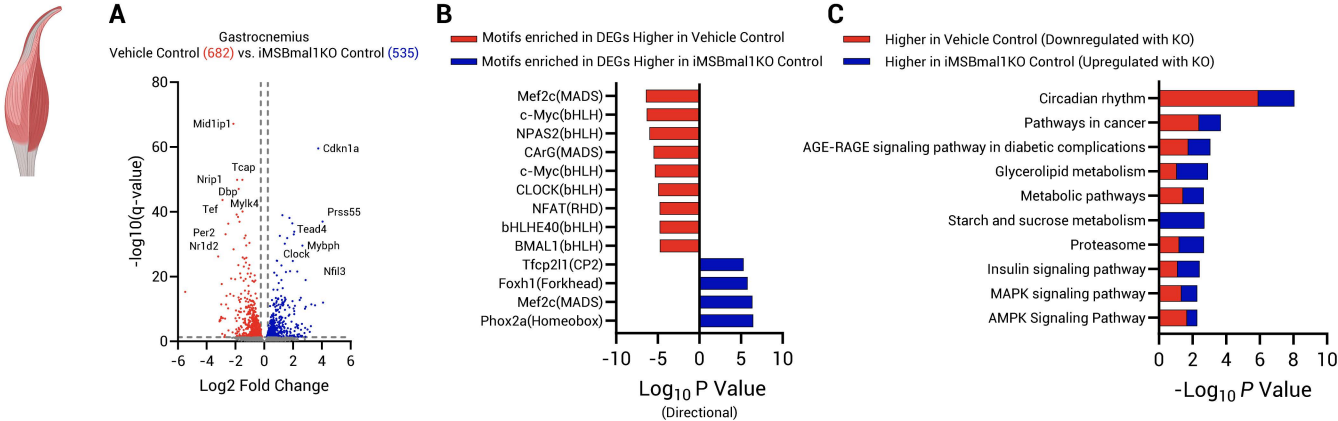
A
Gastrocnemius
Vehicle Control (682) vs. iMSBmal1KO Control (535)
-log10(q-value)
Log2 Fold Change
Mid1ip1
Cdkn1a
Tcap
Nrip1
Dbp
Mylk4
Tef
Prss55
Tead4
Per2
Nr1d2
Mybph
Clock
Nfil3
B
Motifs enriched in DEGs Higher in Vehicle Control
Motifs enriched in DEGs Higher in iMSBmal1KO Control
Mef2c(MADS)
c-Myc(bHLH)
NPAS2(bHLH)
CArG(MADS)
c-Myc(bHLH)
CLOCK(bHLH)
NFAT(RHD)
bHLHE40(bHLH)
BMAL1(bHLH)
Tfcp2l1(CP2)
Foxh1(Forkhead)
Mef2c(MADS)
Phox2a(Homeobox)
Log10 P Value
(Directional)
C
Higher in Vehicle Control (Downregulated with KO)
Higher in iMSBmal1KO Control (Upregulated with KO)
Circadian rhythm
Pathways in cancer
AGE-RAGE signaling pathway in diabetic complications
Glycerolipid metabolism
Metabolic pathways
Starch and sucrose metabolism
Proteasome
Insulin signaling pathway
MAPK signaling pathway
AMPK Signaling Pathway
-Log10 P Value

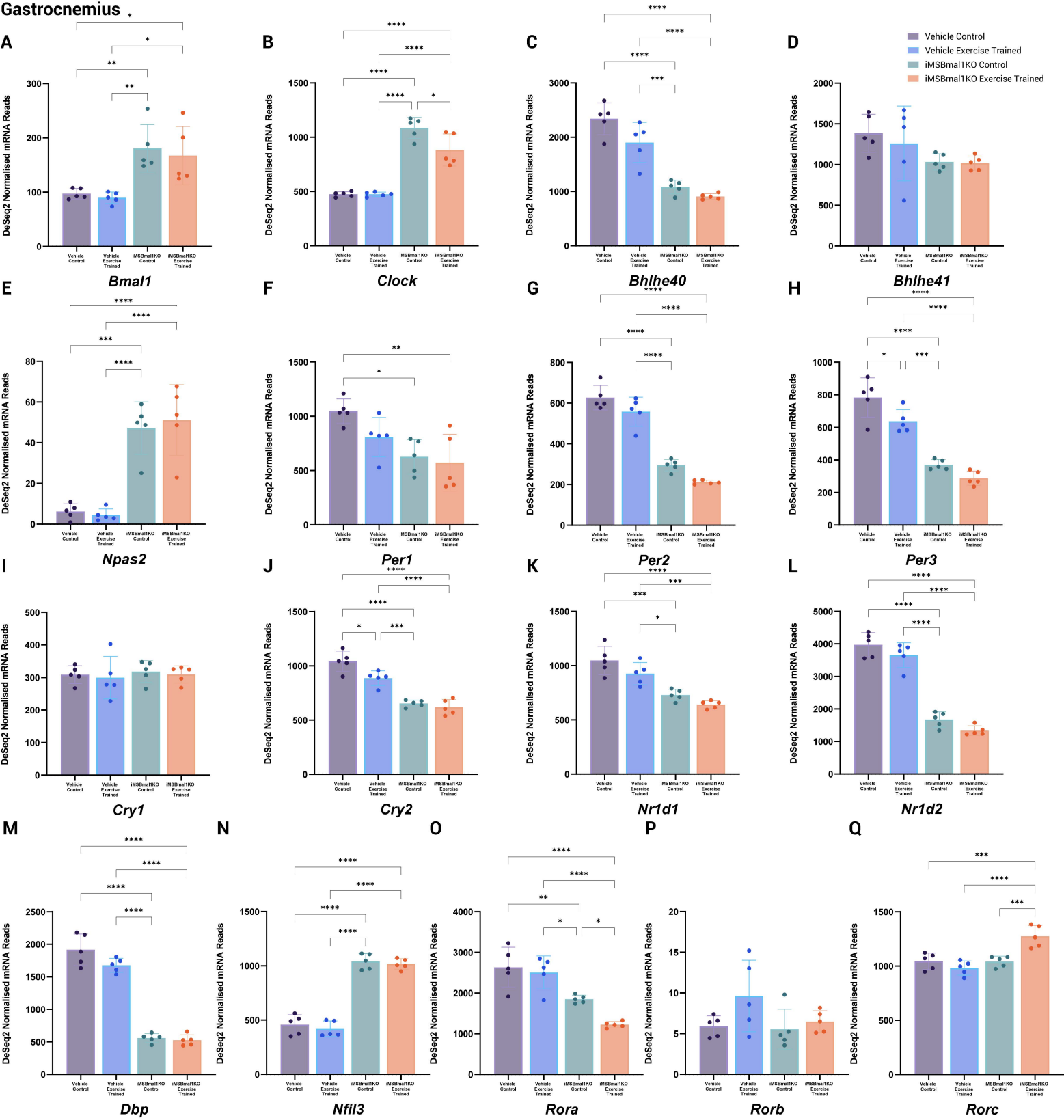
Gastrocnemius
Vehicle Control
Vehicle Exercise Trained
iMSBmal1KO Control
iMSBmal1KO Exercise Trained
DeSeq2 Normalised mRNA Reads
A
Bmal1
B
Clock
C
Bhlhe40
D
Bhlhe41
E
Npas2
F
Per1
G
Per2
H
Per3
I
Cry1
J
Cry2
K
Nr1d1
L
Nr1d2
M
Dbp
N
Nfil3
O
Rora
P
Rorb
Q
Rorc

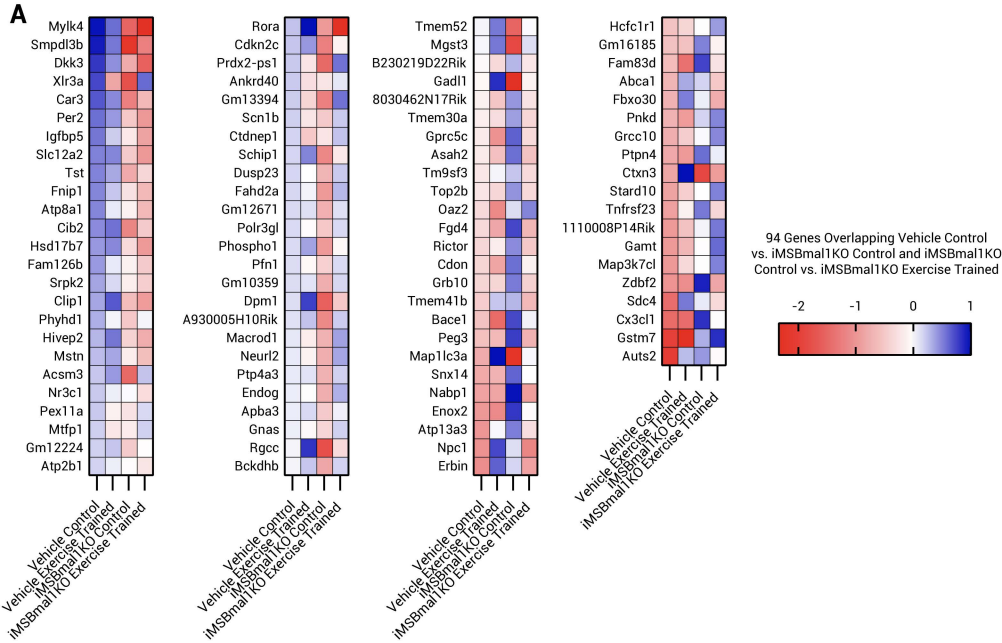
A
Mylk4
Smpdl3b
Dkk3
Xlr3a
Car3
Per2
Igfbp5
Slc12a2
Tst
Fnip1
Atp8a1
Cib2
Hsd17b7
Fam126b
Srpk2
Clip1
Phyhd1
Hivep2
Mstn
Acsm3
Nr3c1
Pex11a
Mtfp1
Gm12224
Atp2b1
Rora
Cdkn2c
Prdx2-ps1
Ankrd40
Gm13394
Scn1b
Ctdnep1
Schip1
Dusp23
Fahd2a
Gm12671
Polr3gl
Phospho1
Pfn1
Gm10359
Dpm1
A930005H10Rik
Macrod1
Neurl2
Ptp4a3
Endog
Apba3
Gnas
Rgcc
Bckdhb
Tmem52
Mgst3
B230219D22Rik
Gadl1
8030462N17Rik
Tmem30a
Gprc5c
Asah2
Tm9sf3
Top2b
Oaz2
Fgd4
Rictor
Cdon
Grb10
Tmem41b
Bace1
Peg3
Map1lc3a
Snx14
Nabp1
Enox2
Atp13a3
Npc1
Erbin
Hcfc1r1
Gm16185
Fam83d
Abca1
Fbxo30
Pnkd
Grcc10
Ptpn4
Ctxn3
Stard10
Tnfrsf23
1110008P14Rik
Gamt
Map3k7cl
Zdbf2
Sdc4
Cx3cl1
Gstm7
Auts2
Vehicle Control
Vehicle Exercise Trained
iMSBmal1KO Control
iMSBmal1KO Exercise Trained
94 Genes Overlapping Vehicle Control vs. iMSBmal1KO Control and iMSBmal1KO Control vs. iMSBmal1KO Exercise Trained
-2
-1
0
1